Small-Angle X-ray Scattering – Interpretation of the results: "What can be obtained from the scattering curve?"

András Wacha

Research Centre for Natural Sciences, Hungarian Academy of Sciences

Outline

Outline

Pinhole camera

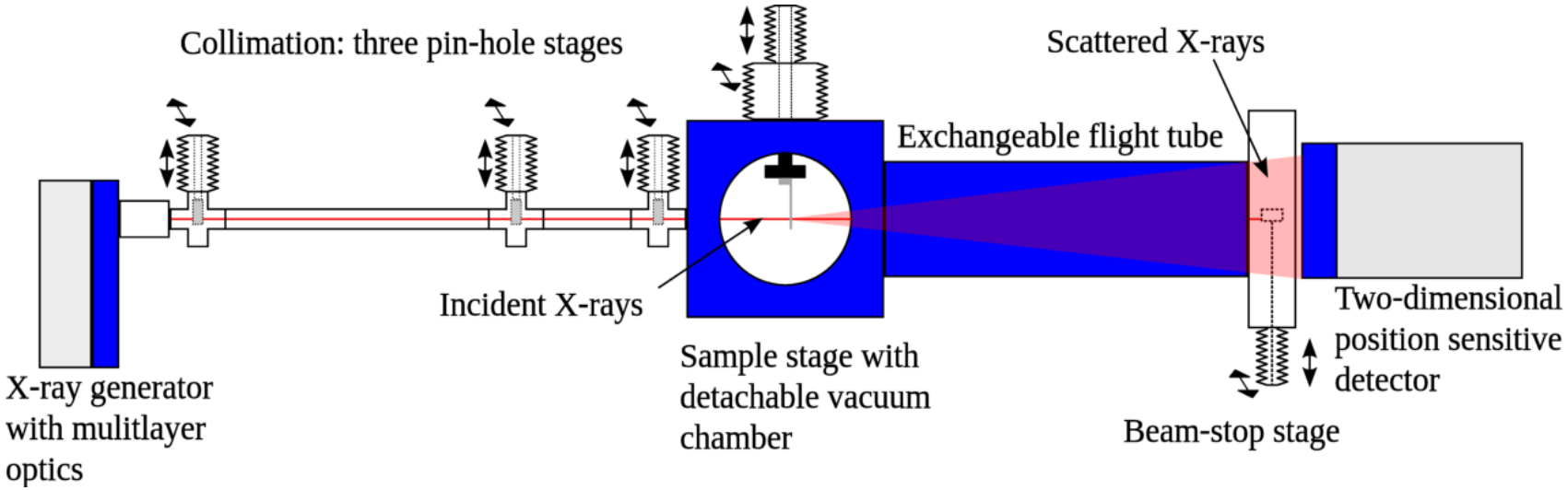

X-ray tube and synchrotron

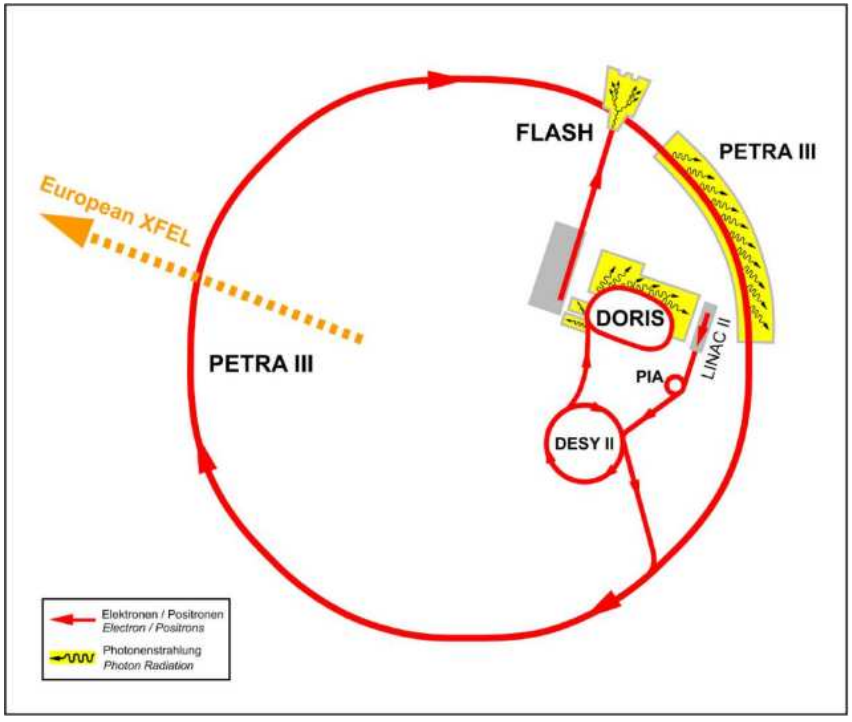

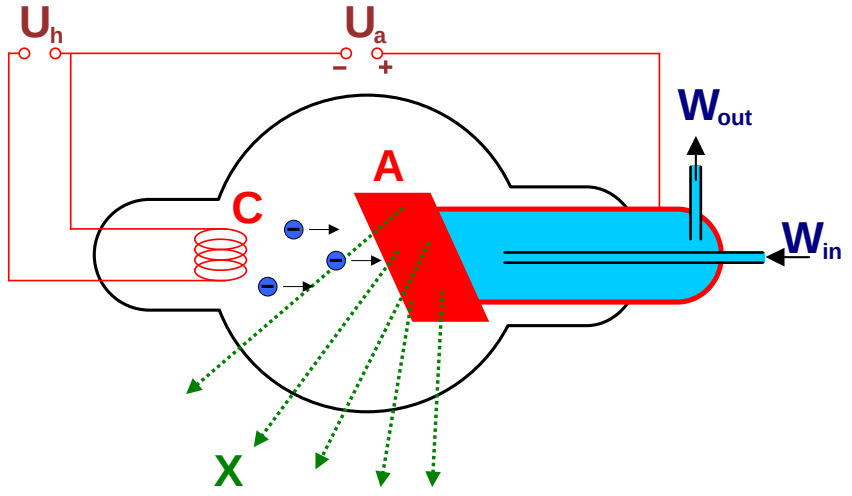

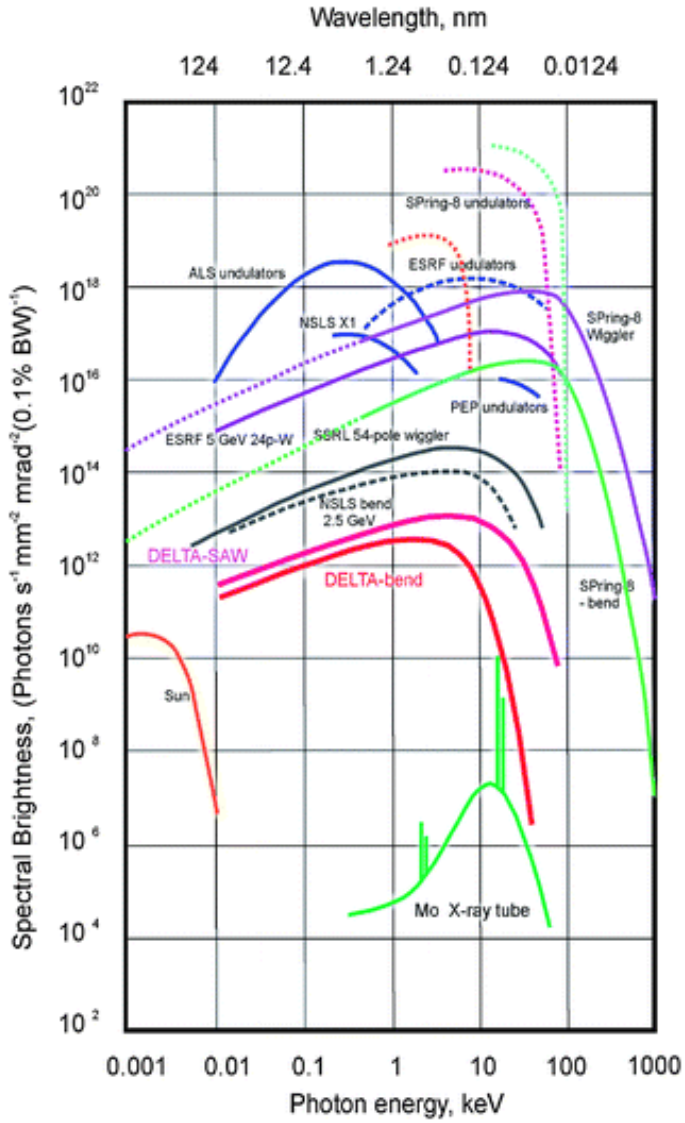

Bragg's law

- Periodic sample (d repeat distance)
- θ incidence and reflection angle
- Constructive interference at the detector: waves reflected from neighbouring planes meet *in phase*
- $\Delta s = n\lambda$ where $n \in \mathbb{N}$
- From geometry: $\Delta s = 2d \sin\theta$
- $2d \sin\theta = n\lambda$
- $\frac{4\pi}{\lambda} \sin\theta = \frac{2\pi}{d} n$
- $\boxed{q = \frac{2\pi}{d} n}$

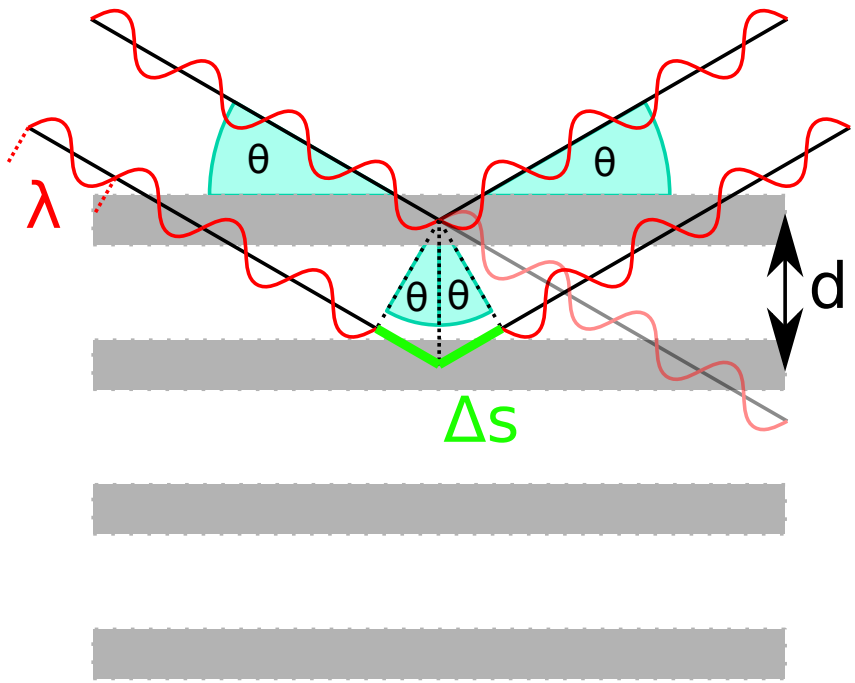

Connection between structure and scattering

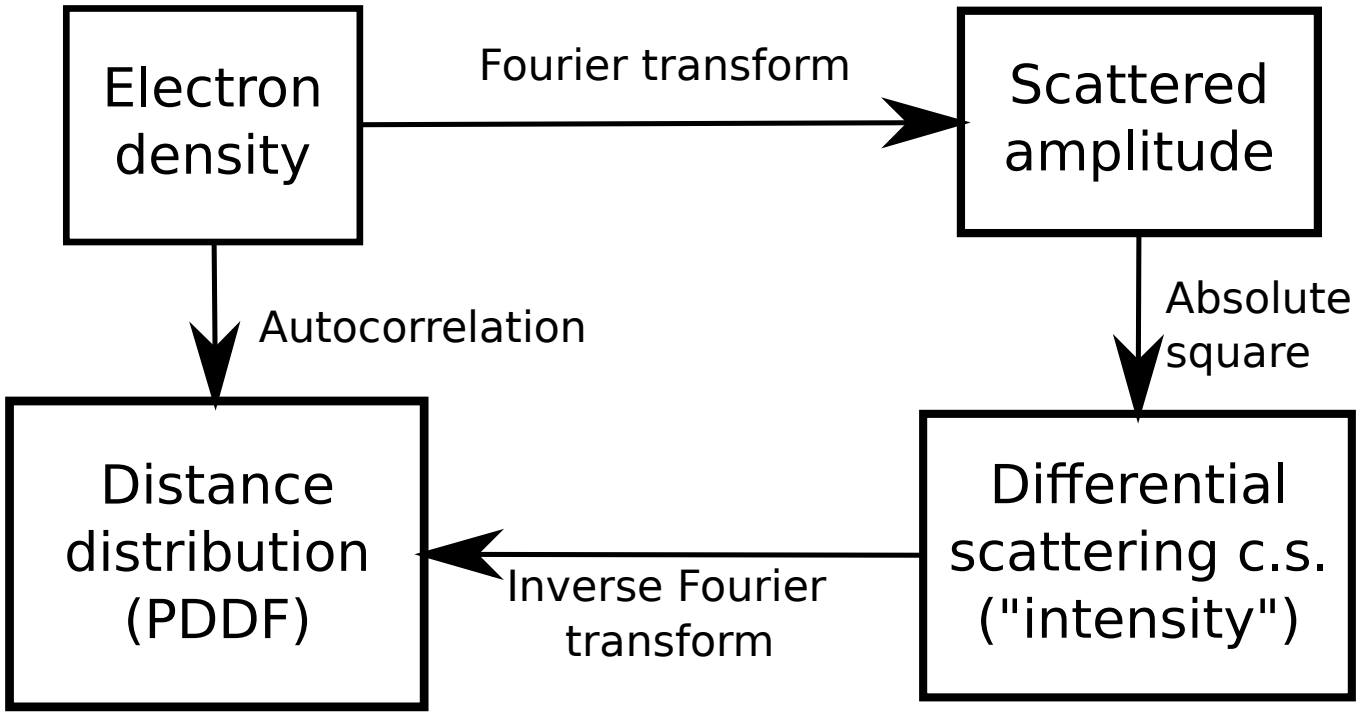

Guinier and Porod limits

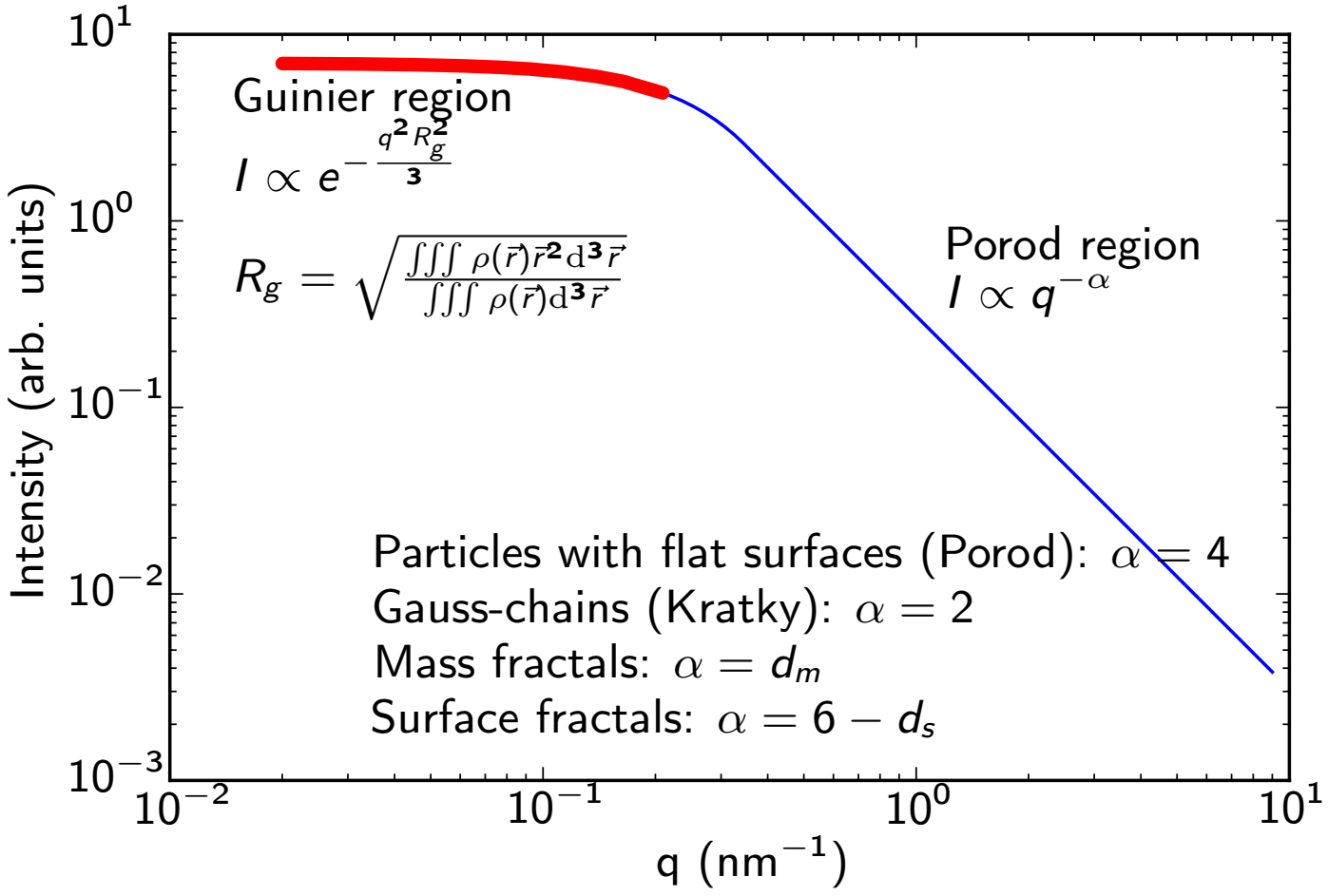

Outline

Lipid systems, liposomes

- Amphipatic molecules: hydrophilic headgroups, hydrophobic carbon chains
- Self-assemble in aqueous solution
- Cell membranes of living organisms
- Other similar molecules: surfactants, detergents etc.
- Application in research & industry:
  - Model membranes
  - Drug carrier vehicles
  - Nanoreactors
  - ...
- Phase transitions
  - Thermotropic
  - Lyotropic

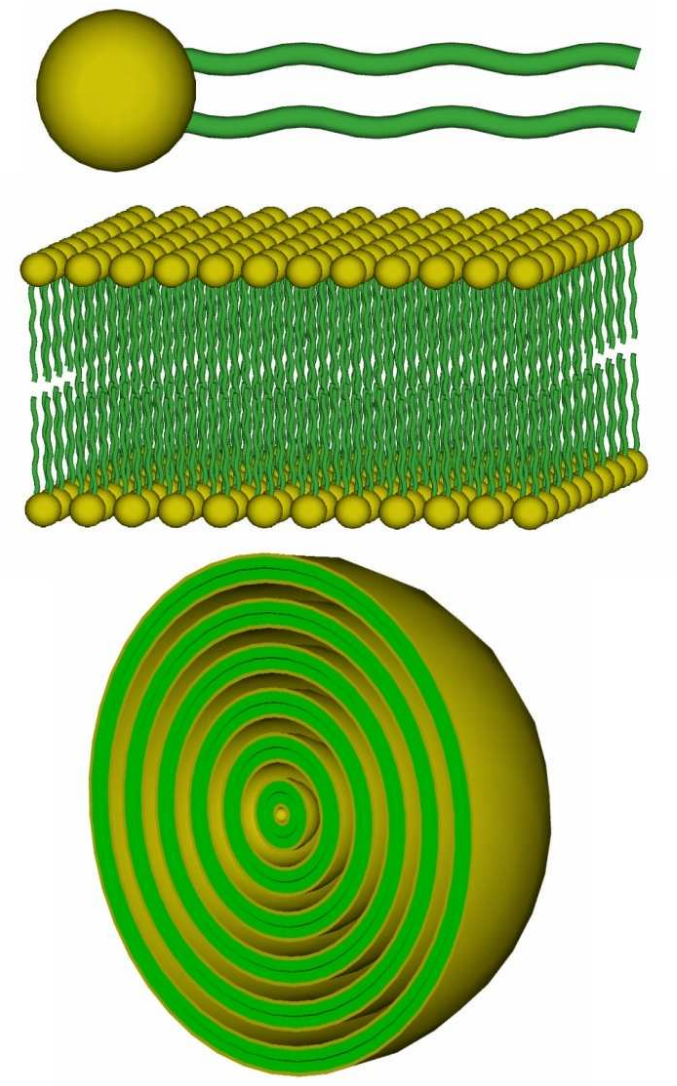

Self-assembled structures of phospholipid systems

- The self-assembled structure is determined by:
  - Shape of the lipid molecule
  - Length and flexibility of the carbon chains
  - Electrostatic charge of the headgroups
- Bilayer lipids: approximately cylindrical
- Non-bilayer lipids: conical shape
  - Large headgroup cross-section area: micelle / hexagonal phase
  - Small headgroup cross-section area inverse micelle / inverse hexagonal phase

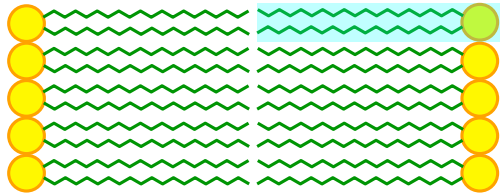

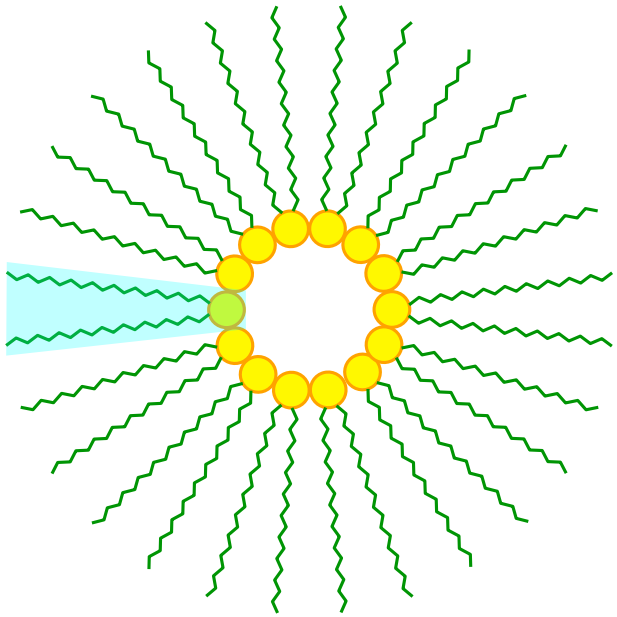

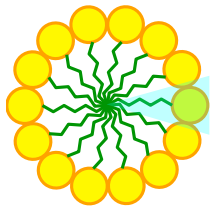

Self-assembled structures of phospholipid systems

- The self-assembled structure is determined by:
  - Shape of the lipid molecule
  - Length and flexibility of the carbon chains
  - Electrostatic charge of the headgroups
- Bilayer lipids: approximately cylindrical
- Non-bilayer lipids: conical shape
  - Large headgroup cross-section area: micelle / hexagonal phase
  - Small headgroup cross-section area inverse micelle / inverse hexagonal phase

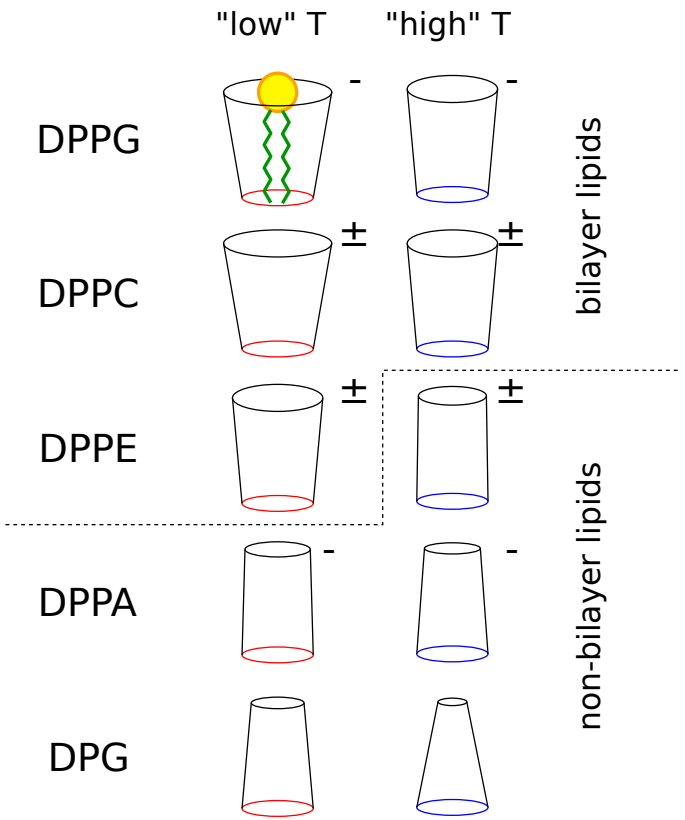

Lyotropic phases of lipid/water systems

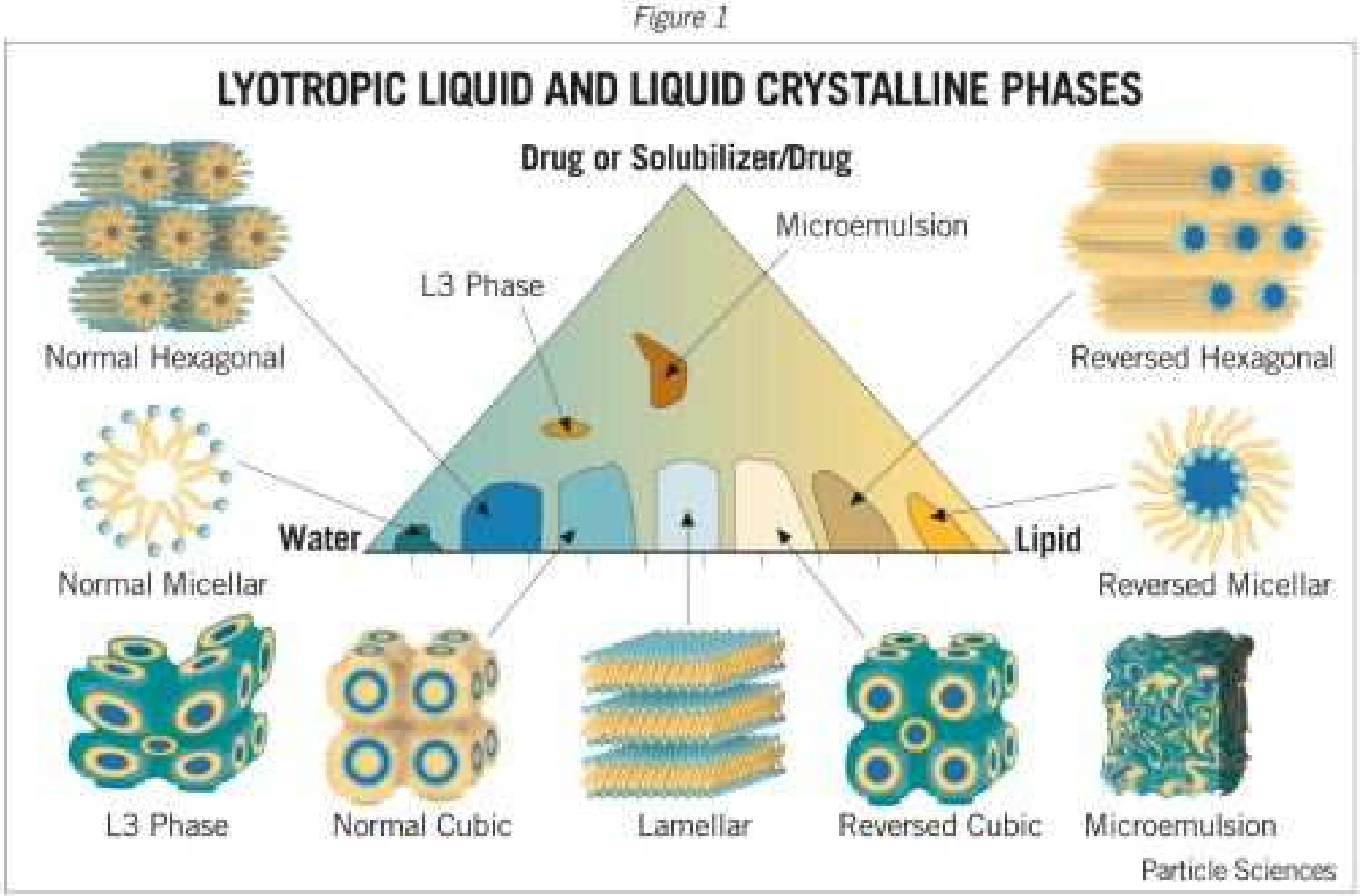

Thermotropic phases of DPPC/water mixtures

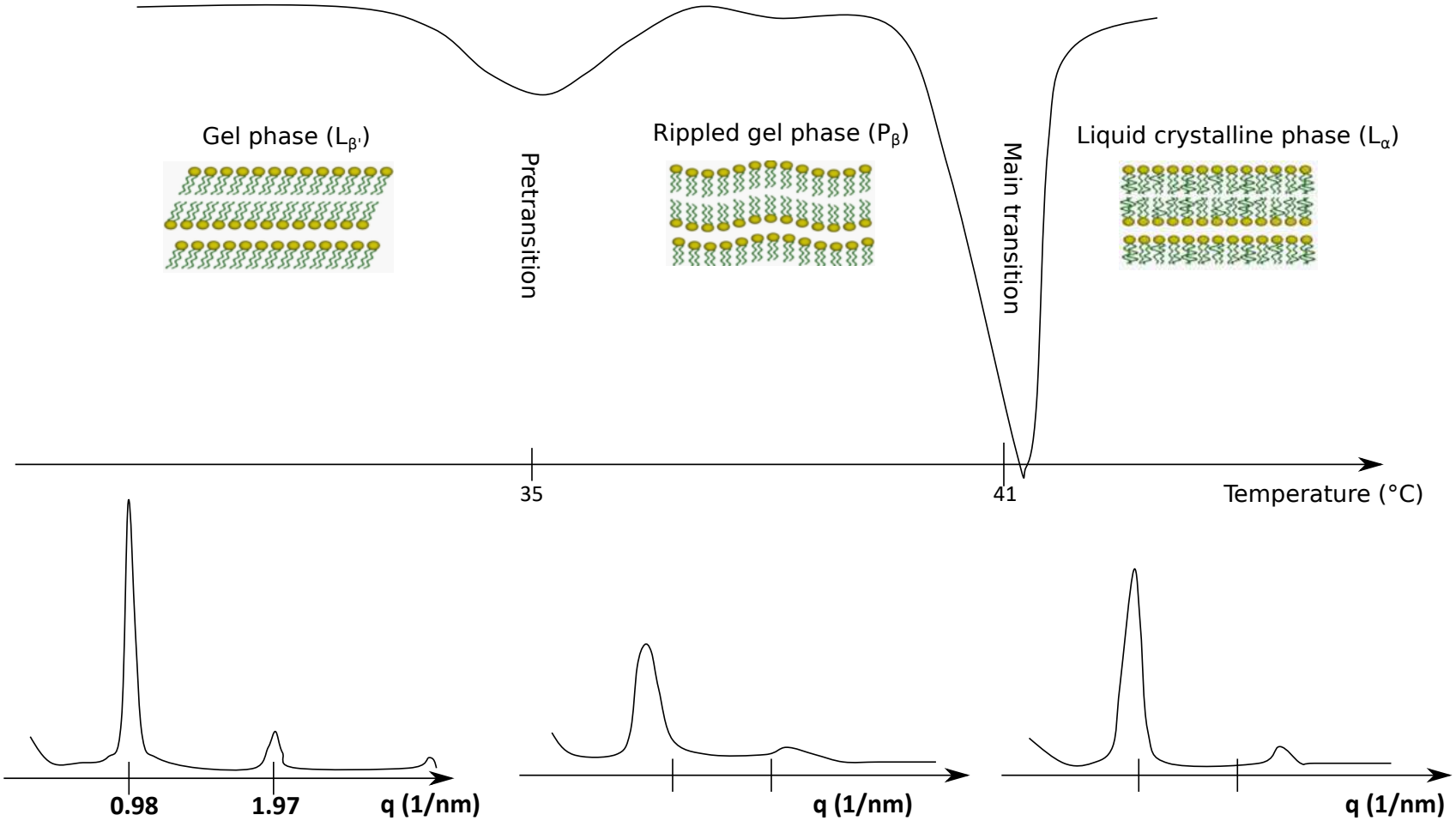

Thermotropic phases of DPPC: SAXS

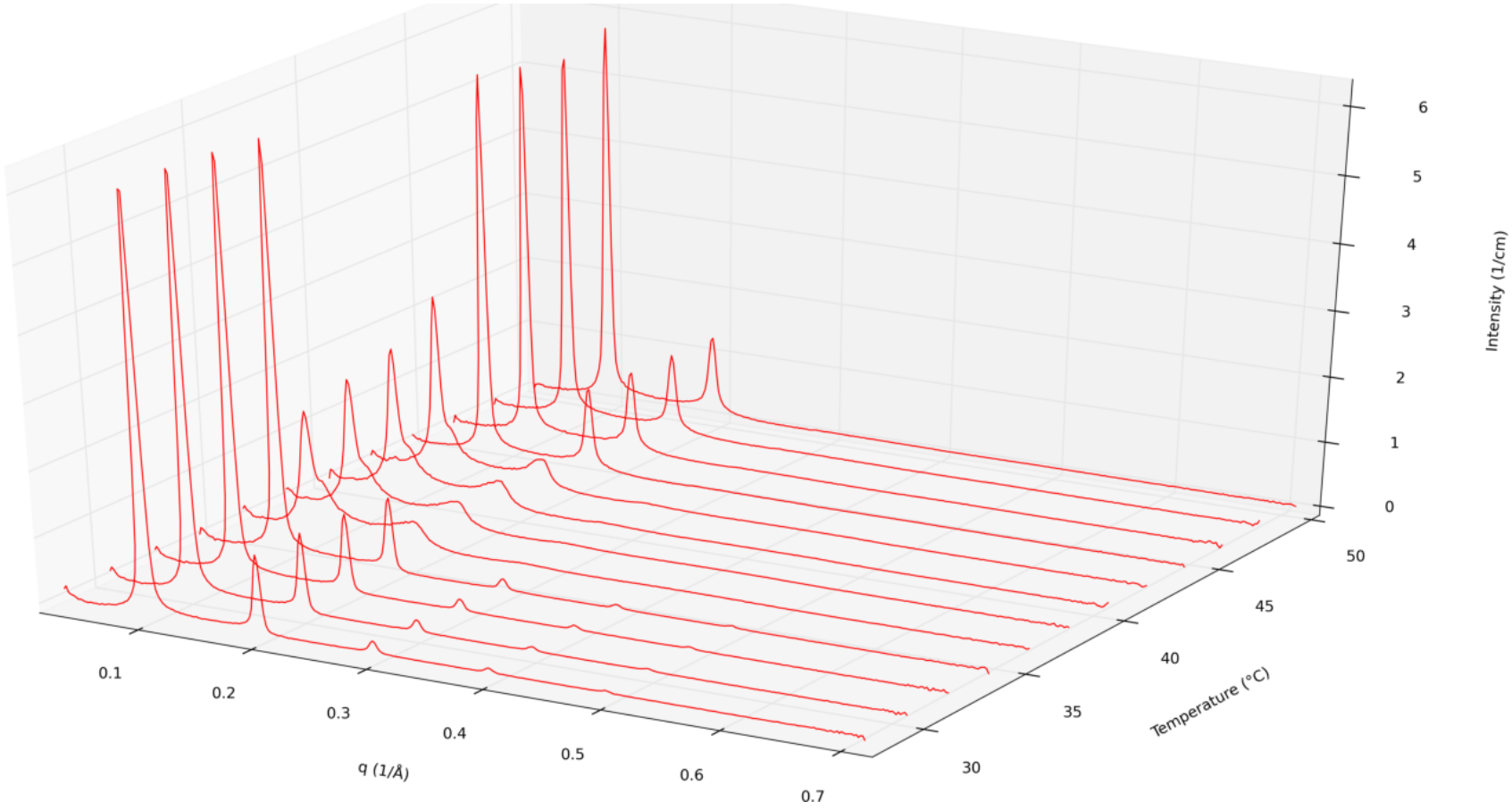

Relative peak positions: 1, 2, 3, 4 $\rightarrow$ lamellar

Thermotropic phases of DPPC: SAXS

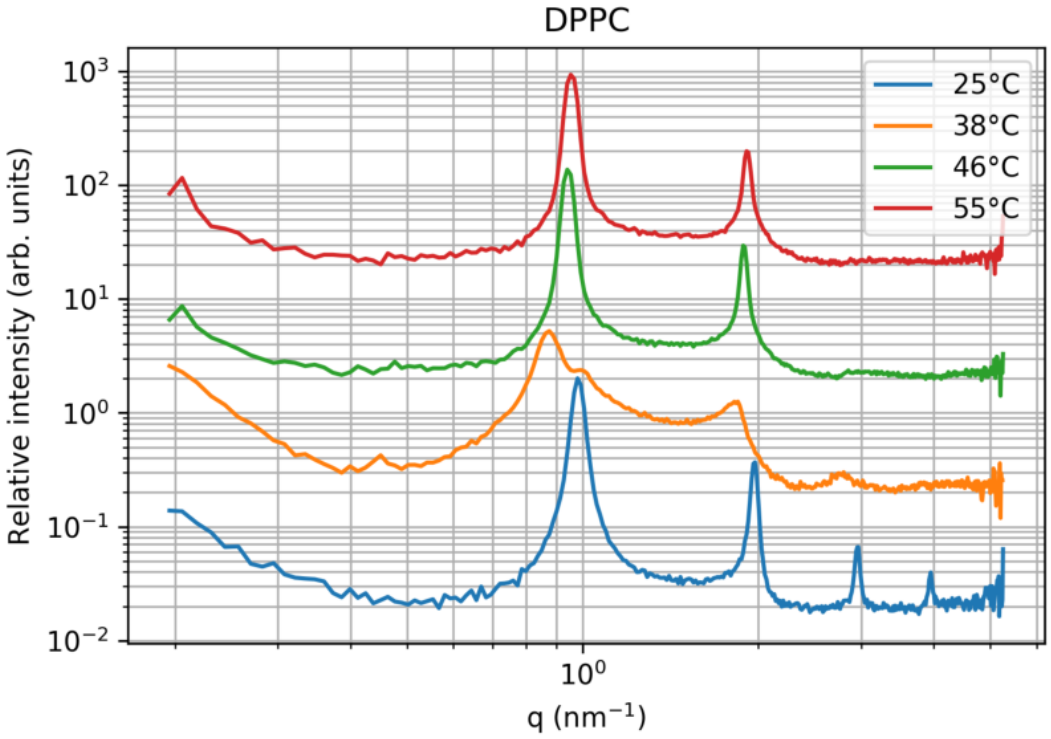

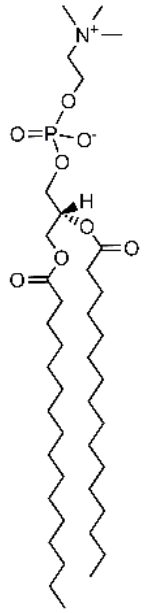

Relative peak positions: 1, 2, 3, 4 $\rightarrow$ lamellar

Temperature	25°C	38°C	46°C	55°C
Phase	L_β	$P_{\beta'}$	L_α	L_α
Repeat distance	6.373 nm	"7.193 nm*"	6.657 nm	6.569 nm

DOPC

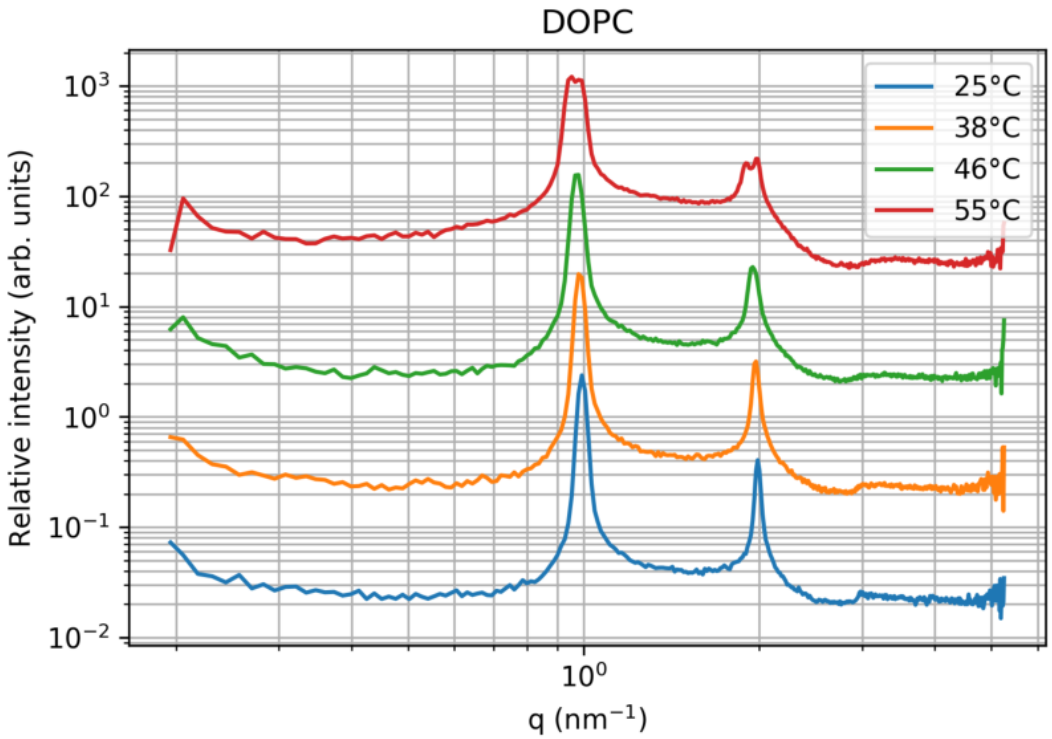

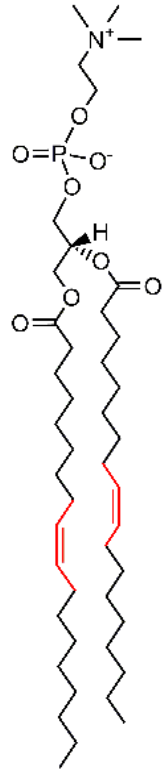

Relative peak positions: 1, 2, (3)

Temperautre	25°C	38°C	46°C	55°C
Phase	L_α	L_α	L_α	L_α
Repeat distance	6.323 nm	6.370 nm	6.440 nm	6.642 nm
				6.335 nm

DOPE: hexagonal phase

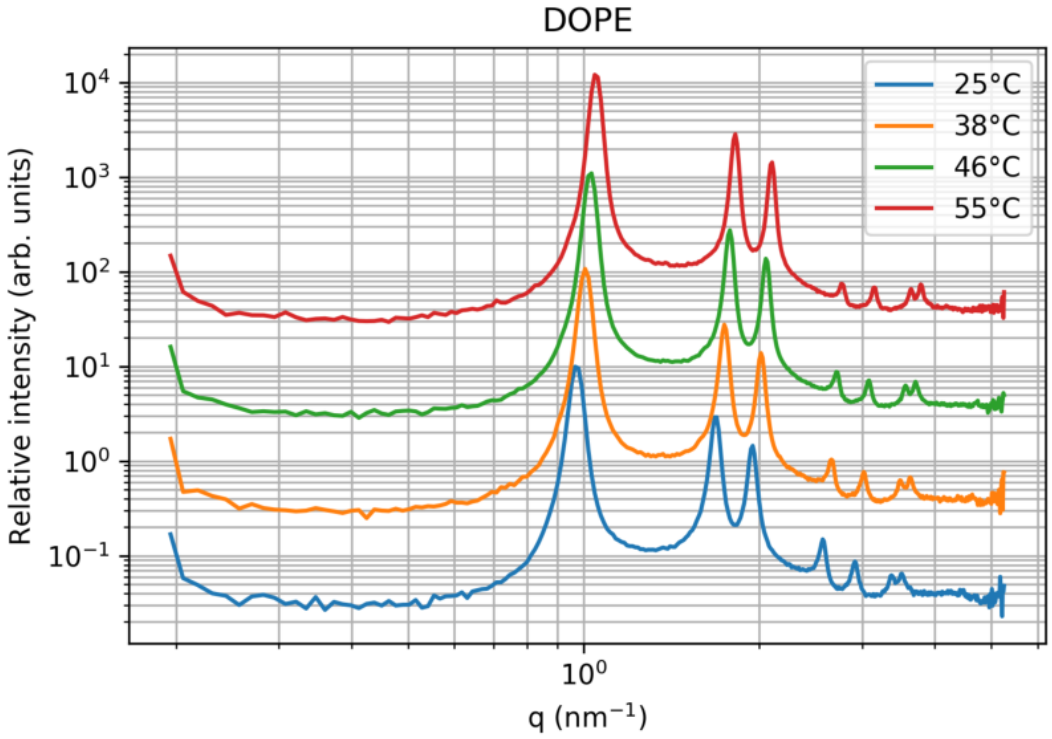

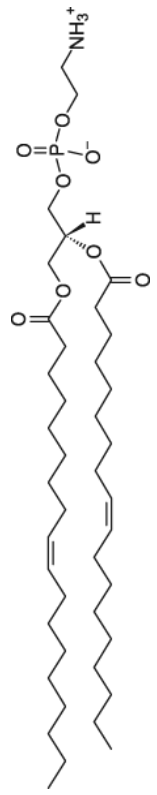

Relative peak positions: $1, \sqrt{3}, 2, \sqrt{7}, 3, \sqrt{12}, \sqrt{13}$

Temperature	25°C	38°C	46°C	55°C
Phase	H_{II}	H_{II}	H_{II}	H_{II}
Lattice parameter	6.458 nm	6.244 nm	6.119 nm	5.989 nm

Coexistence of phases

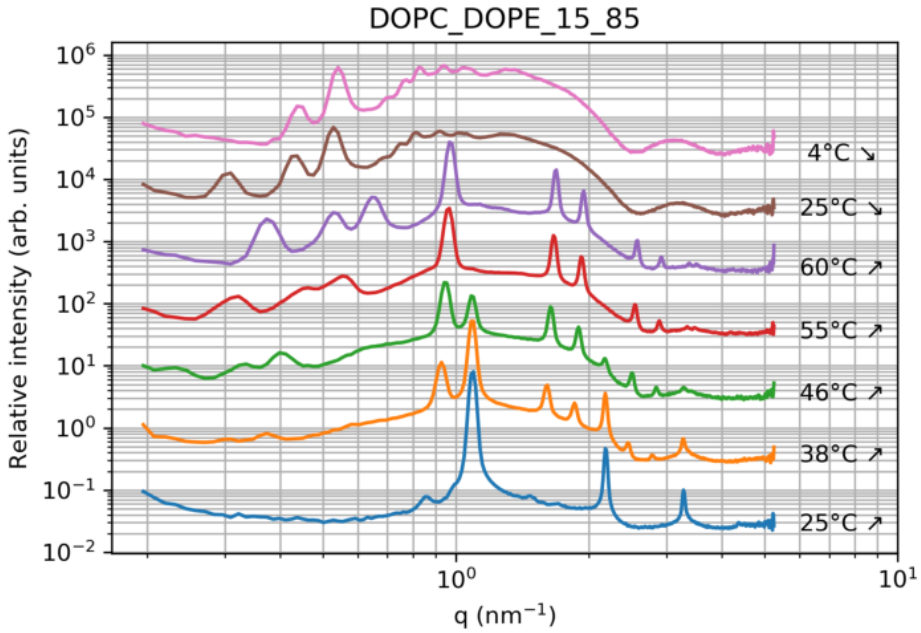

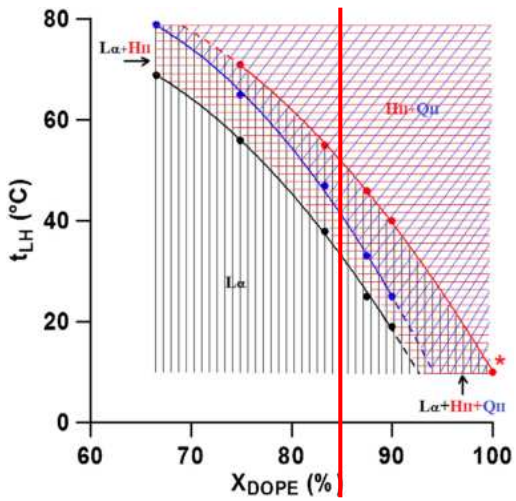

- Room temperature: lamellar phase (L_α)
- 38 °C: appearance of the inverse hexagonal phase (H_{II})
- 46 °C: the cubic phase (Q_{II}) appears, three phases coexist
- 55 °C: the lamellar phase vanishes
- after cooling: the cubic phase remains, the lamellar phase is not recovered: memory effect!

Sterically stabilized unilamellar vesicles

- Unilamellar vesicle: a single phospholipid bilayer
- Hydration of lipids: multilamellar vesicles are formed *spontaneously*
- "Unilamellarization": ultrasound threatment / extrusion
- Avoiding spontaneous fusion to multilamellar vesicles:
  - Charged lipids
  - Sterical stabilization: e.g. with PEG-conjugated lipids
- Primary application: drug carrier and targeting agents $\Rightarrow$ size is critical!

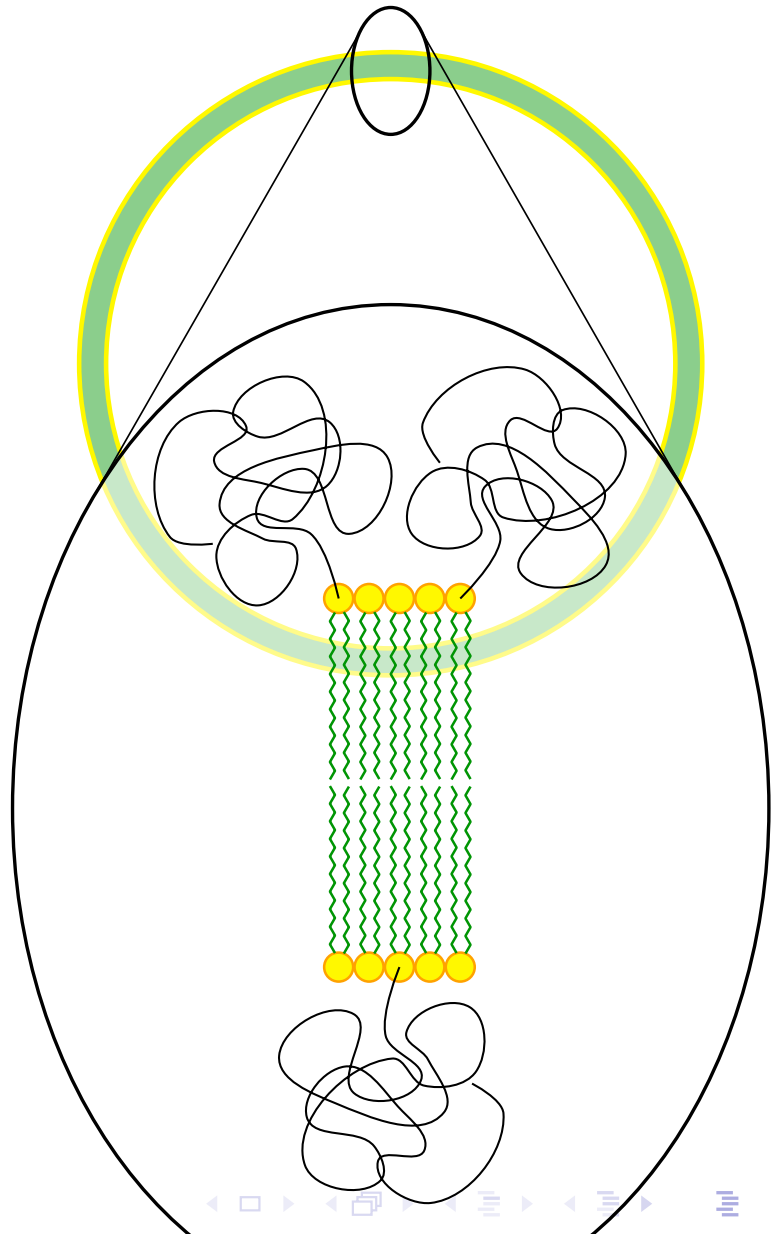

Sterically stabilized vesicles

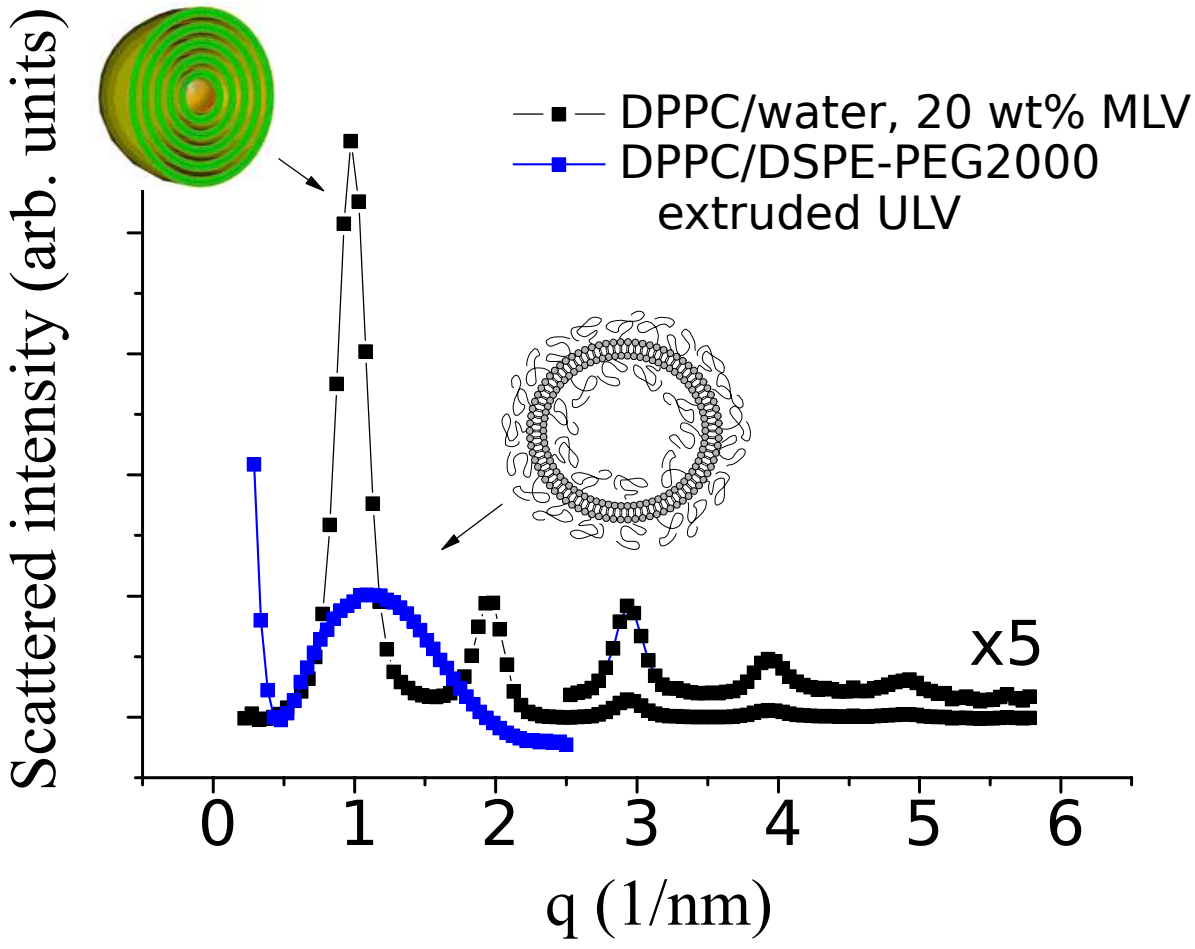

- Less electrons in the object $\Rightarrow$ weaker scattering
- No layer-layer correlation $\Rightarrow$ no peaks
- What we see is the *phospholipid bilayer form factor*

Scattering of a phospholipid bilayer

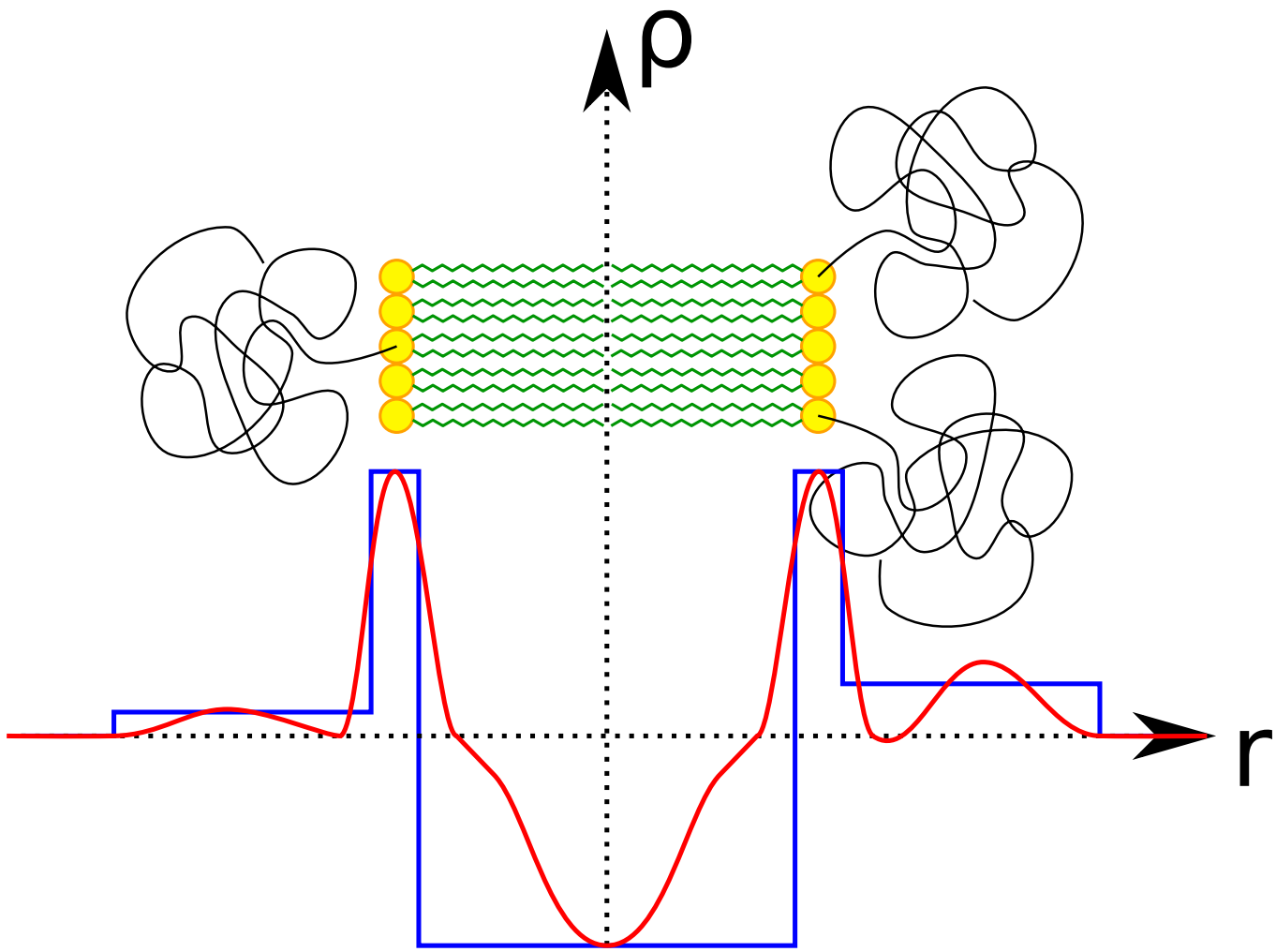

$$I_{\mathrm{SSL}}(q) = [F_{\mathrm{PEG,in}}(q) + F_{\mathrm{head,in}}(q) + F_{\mathrm{CH}}(q) + F_{\mathrm{head,out}}(q) + F_{\mathrm{PEG,out}}(q)]^2$$

Scattering of a bilayer

$$I_{SSL}(q) = [F_{PEG,in}(q) + F_{head,in}(q) + F_{CH}(q) + F_{head,out}(q) + F_{PEG,out}(q)]^2$$

- Every term is a step function or a Gaussian curve
- $\rho(q) = \begin{cases} \rho_0 & \text{if } |r - r_0| < \sigma \\ 0 & \text{otherwise} \end{cases}$ $\rho(q) = \frac{\rho_0}{\sqrt{2\pi\sigma^2}} e^{-\frac{(r-r_0)^2}{2\sigma^2}}$
- Model parameters:

	ρ	r	σ
Inner PEG	$\rho_{PEG,in}$	$r_{PEG,in}$	$\sigma_{PEG,in}$
Inner headgroup	ρ_{head}	$-r_{head}$	σ_{head}
Carbon chain	-1	0	σ_{tail}
Outer headgroup	ρ_{head}	r_{head}	σ_{head}
Outer PEG	$\rho_{PEG,out}$	$r_{PEG,out}$	$\sigma_{PEG,out}$

  + global intensity scaling factor (A) + constant background (C) + mean vesicle radius (R_0) + spread of the vesicle radius (δR)
- Asymmetric model (PEGs are different): 14 parameters
- Symmetric model (PEGs are equivalent): 11 parameters

Sterically stabilized vesicles

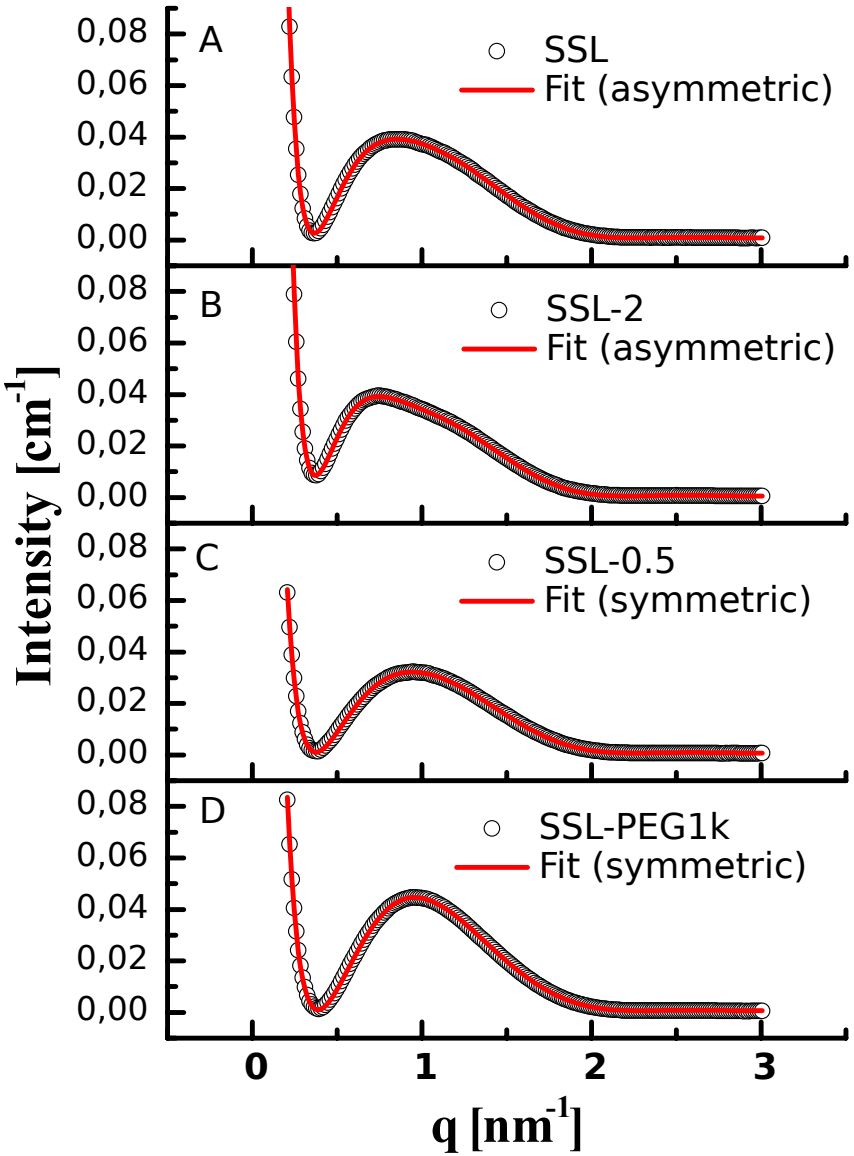

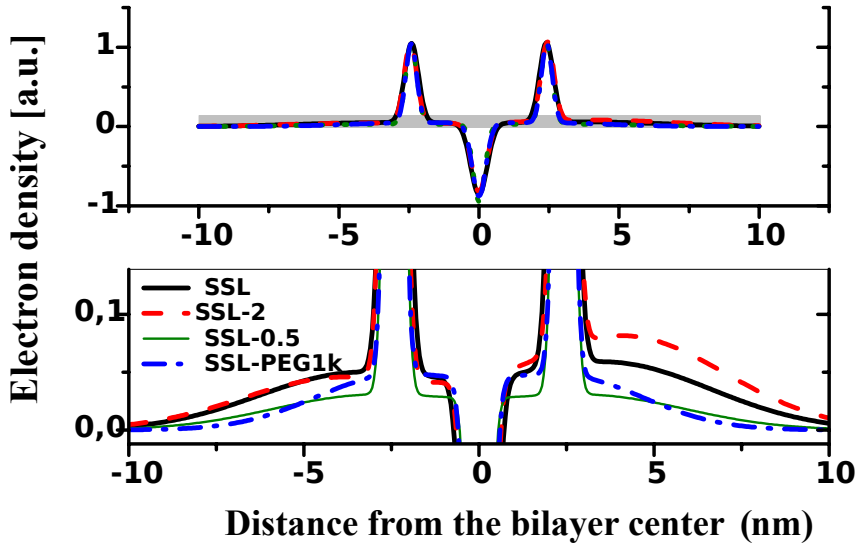

SSL: HSPC + DSPE-PEG2000

SSL-2: HSPC + 2×DSPE-PEG2000

SSL-0.5: HSPC + 0.5×DSPE-PEG2000

SSL-PEG1k: HSPC + DSPE-PEG1000

Micelles

- Self-assembling systems composed of amphipatic molecules
- Conical shape: large hydrophilic head, narrow hydrophobic tail
- Critical micelle concentration (CMC)
- Not only spherical (even when only one component!)

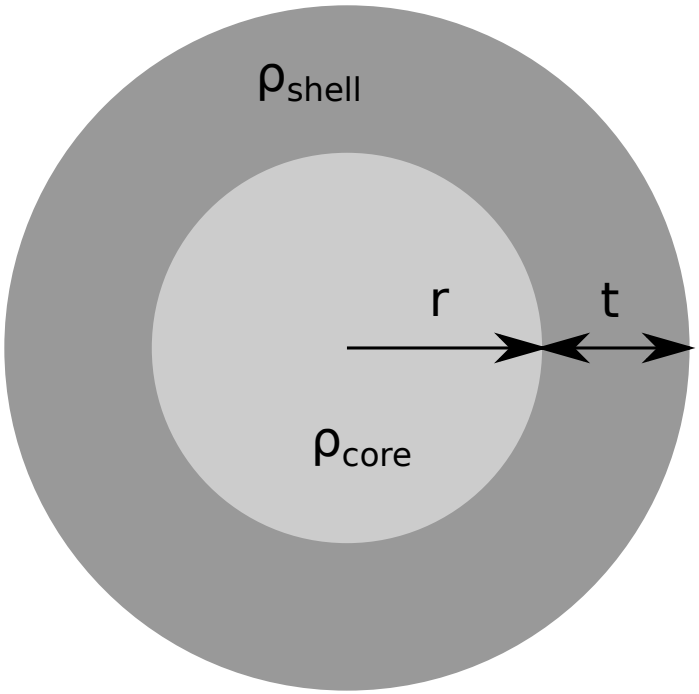

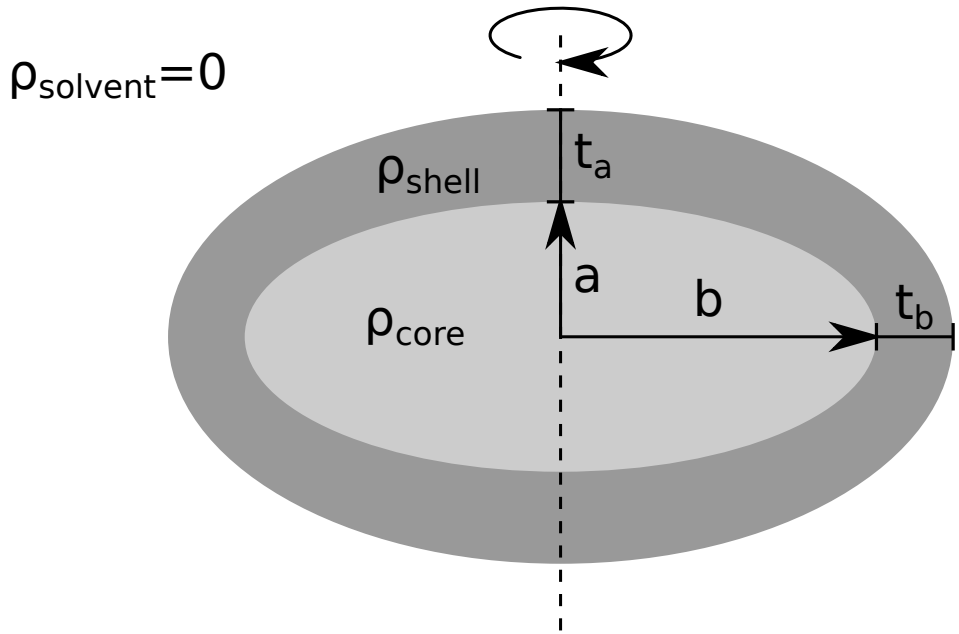

Bicelles

- Two components: long-chained bilayer lipid and short-chained detergent
- The shape is controlled by:
  $q = c_{\text{lipid}} / c_{\text{detergens}}$
  - $q = 0$: detergent micelle
  - $q \to \infty$: bilayer
- Importance: small carriers for membrane proteins
- Typical example: DHPC-DMPC bicelle
  - DHPC: 1,2-Dihexanoyl-sn-Glycero-3-Phosphocholine
  - DMPC: 1,2-Dimyristoyl-sn-Glycero-3-Phosphocholine

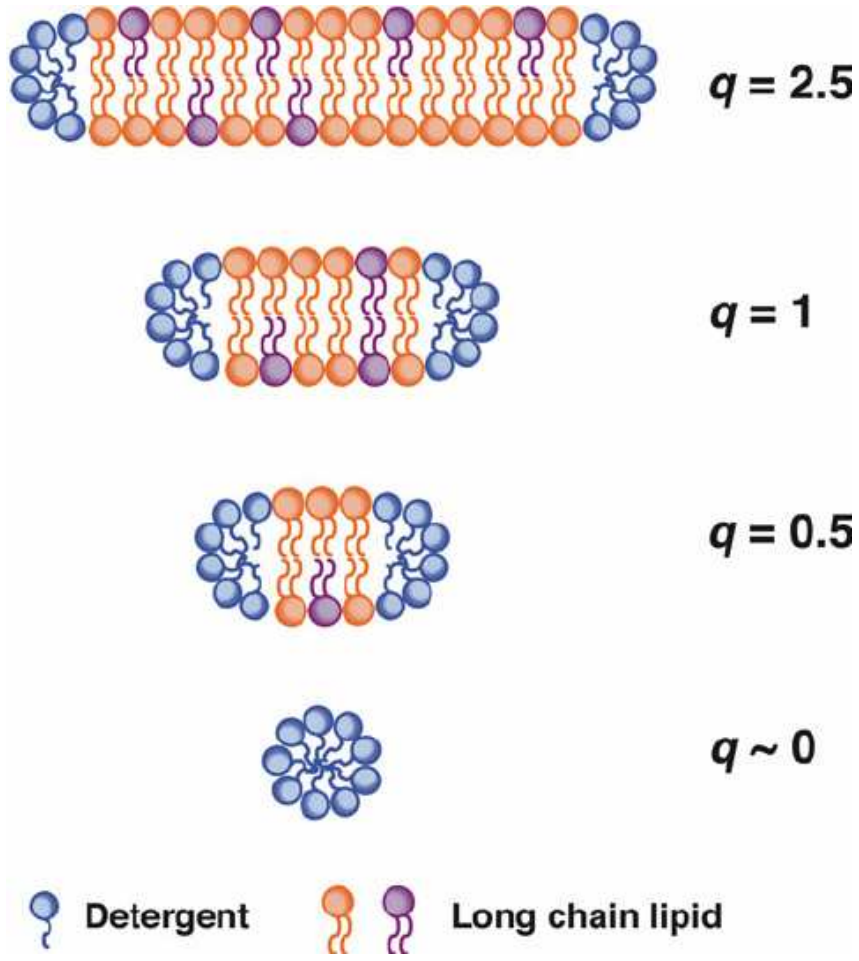

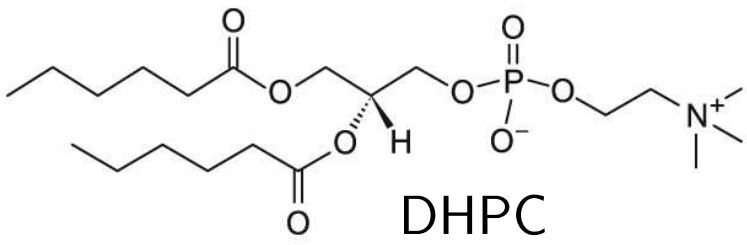

DHPC

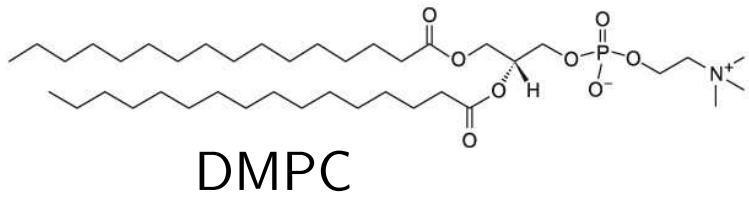

DMPC

Scattering of a DHPC micelle

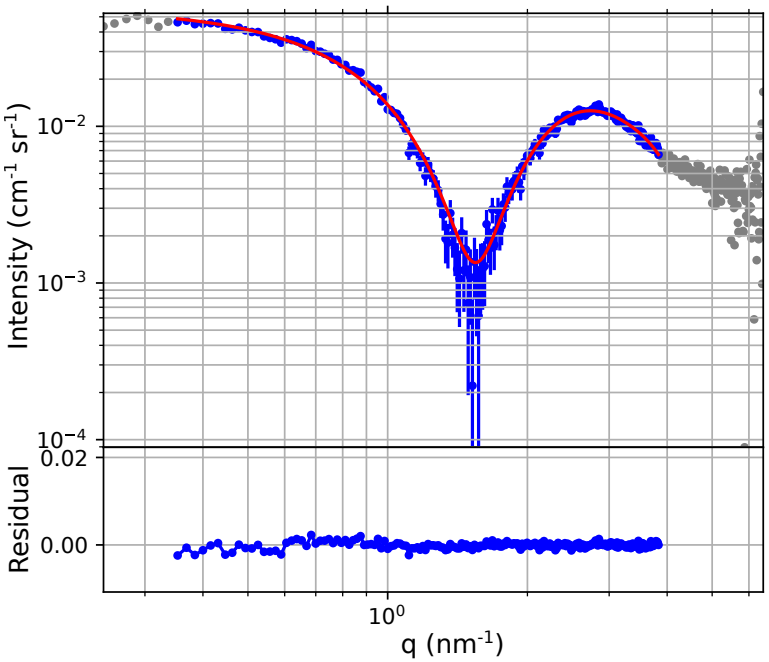

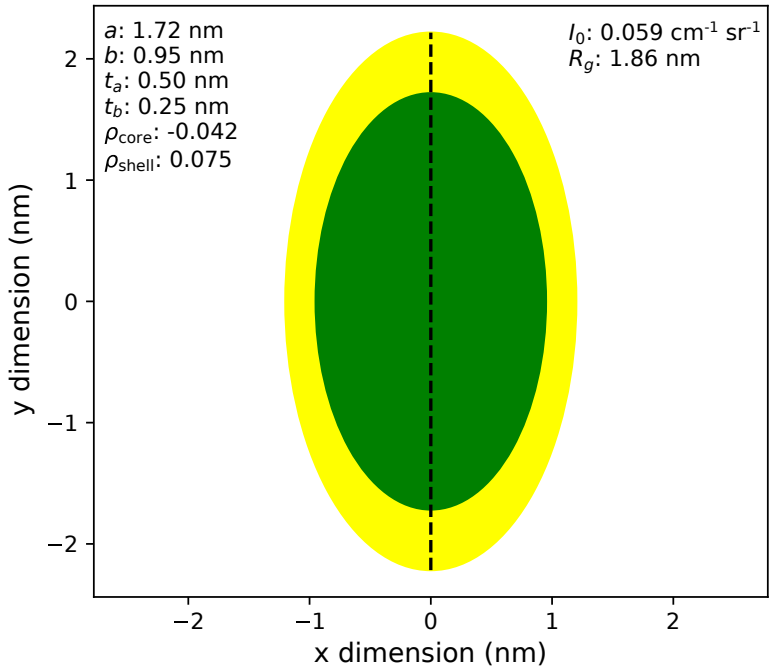

- Scattering: similar to the lipid bilayers
- Guinier region
- Fitting: micelle shape

Peptide-carrying DHPC-DMPC bicelles

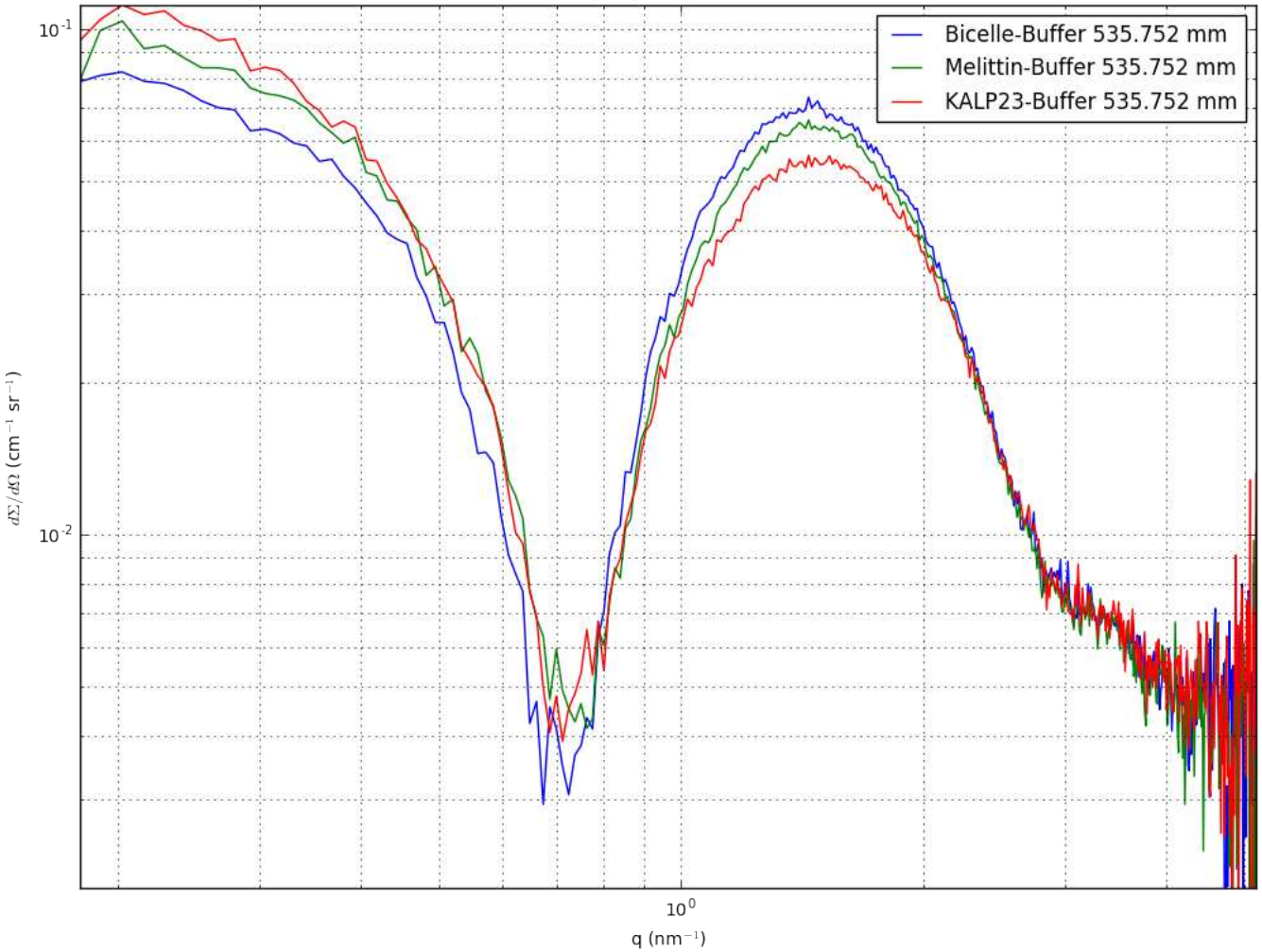

Outline

Activated carbons

Activated carbons

- Adsorbent, substrate, structural material
- Hierarchical structure
- Preparation:
  1. Pyrolysis: organic $\rightarrow$ C
  2. Activation: pore formation
- Tailorable
  - choice of the precursor
  - parameters of the activation
- Anisotropy: not utilized (but could be...)

Model of the hierarchical structure

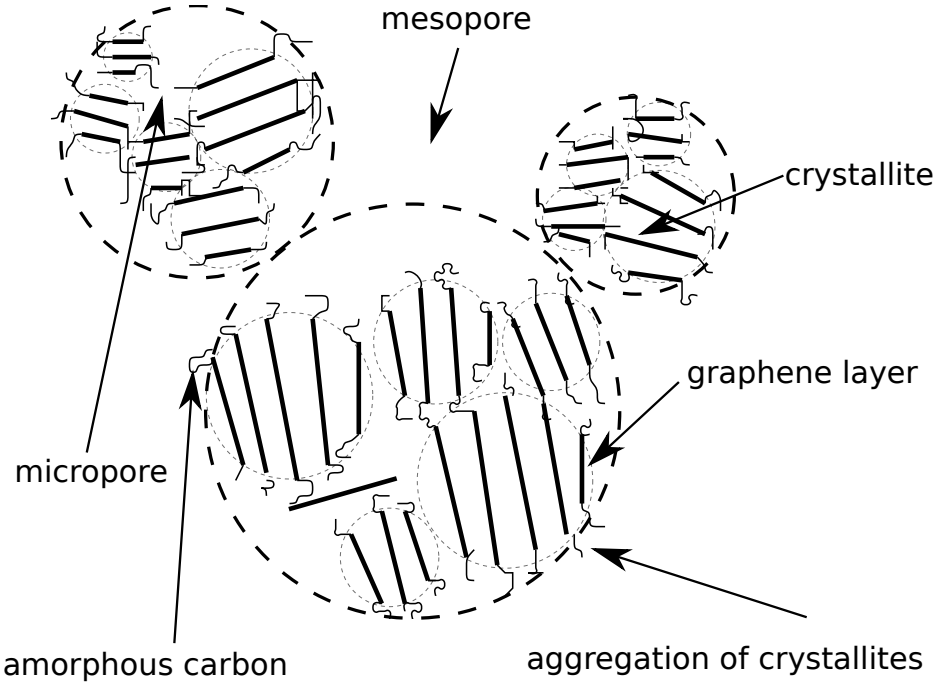

Hirsch, Proc. Royal Soc. Lond. A (1954) 226(1165) 143-169

Activated carbons

Activated carbons

- Adsorbent, substrate, structural material
- Hierarchical structure
- Preparation:
  1. Pyrolysis: organic $\rightarrow$ C
  2. Activation: pore formation
- Tailorable
  - choice of the precursor
  - parameters of the activation
- Anisotropy: not utilized (but could be...)

Model of the hierarchical structure

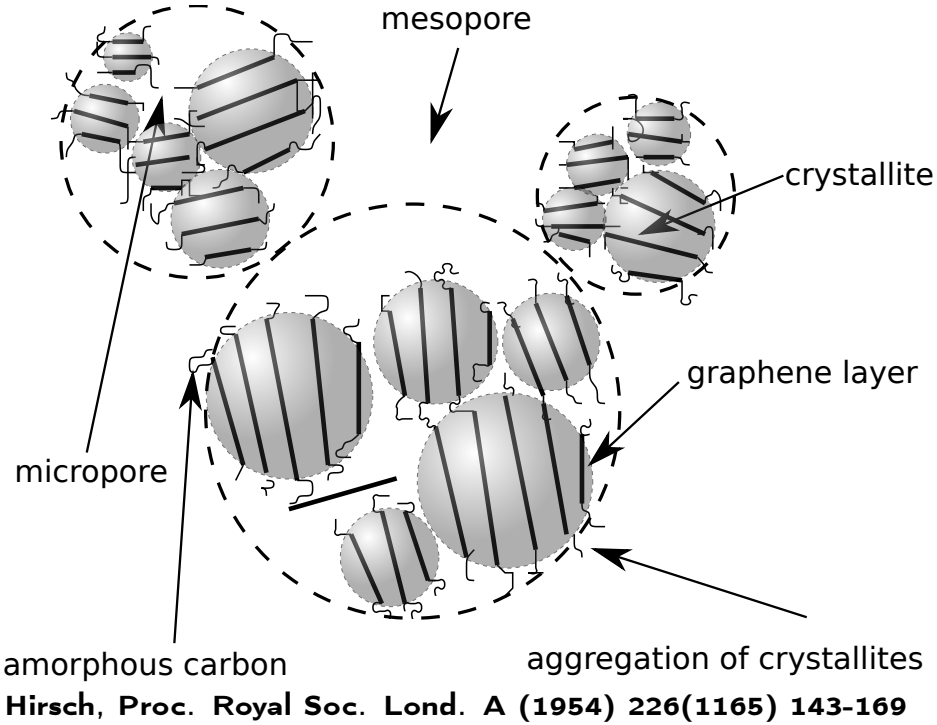

Hirsch, Proc. Royal Soc. Lond. A (1954) 226(1165) 143-169

Activated carbons

Activated carbons

- Adsorbent, substrate, structural material
- Hierarchical structure
- Preparation:
  1. Pyrolysis: organic $\rightarrow$ C
  2. Activation: pore formation
- Tailorable
  - choice of the precursor
  - parameters of the activation
- Anisotropy: not utilized (but could be...)

Model of the hierarchical structure

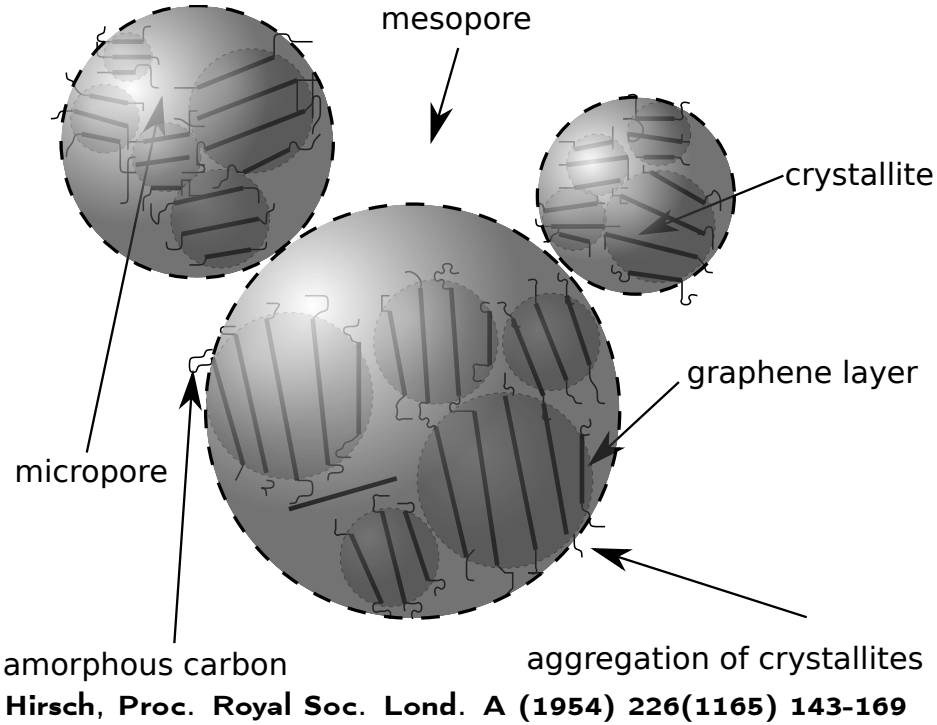

Hirsch, Proc. Royal Soc. Lond. A (1954) 226(1165) 143-169

Sample preparation

Sample preparation for SAXS measurements

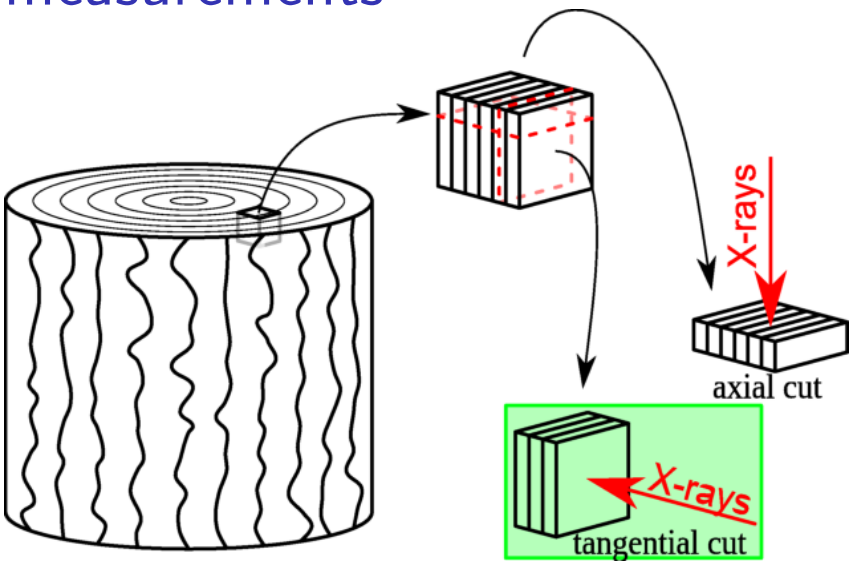

- Pyrolysis of 1 cm^3 wooden cubes (700 °C) $\rightarrow$ $6 \times 6 \times 6$ mm^3 carbon cubes
- Physical activation:
  $C_{(s)} \xrightarrow[900^\circ C]{H_2O_{(g)}} C_{(g)}$
- Mass decrease (conversion) with increasing activation time:

	Fagus sylvatica (beech)	Quercus robur (oak)	Picea abies (spruce)
0 min	0%	0 %	0 %
15 min	9 %	10 %	10 %
45 min	26 %	26 %	27 %
90 min	54 %	55 %	49 %

- SAXS measurements: synchrotron beamlines (Hamburg, Berlin)

For details, see: Wacha, Varga, Vainio, Hoell, Bóta (2011) Carbon 49(12) 3958-3971.

SAXS on activated carbons

Tangential cut

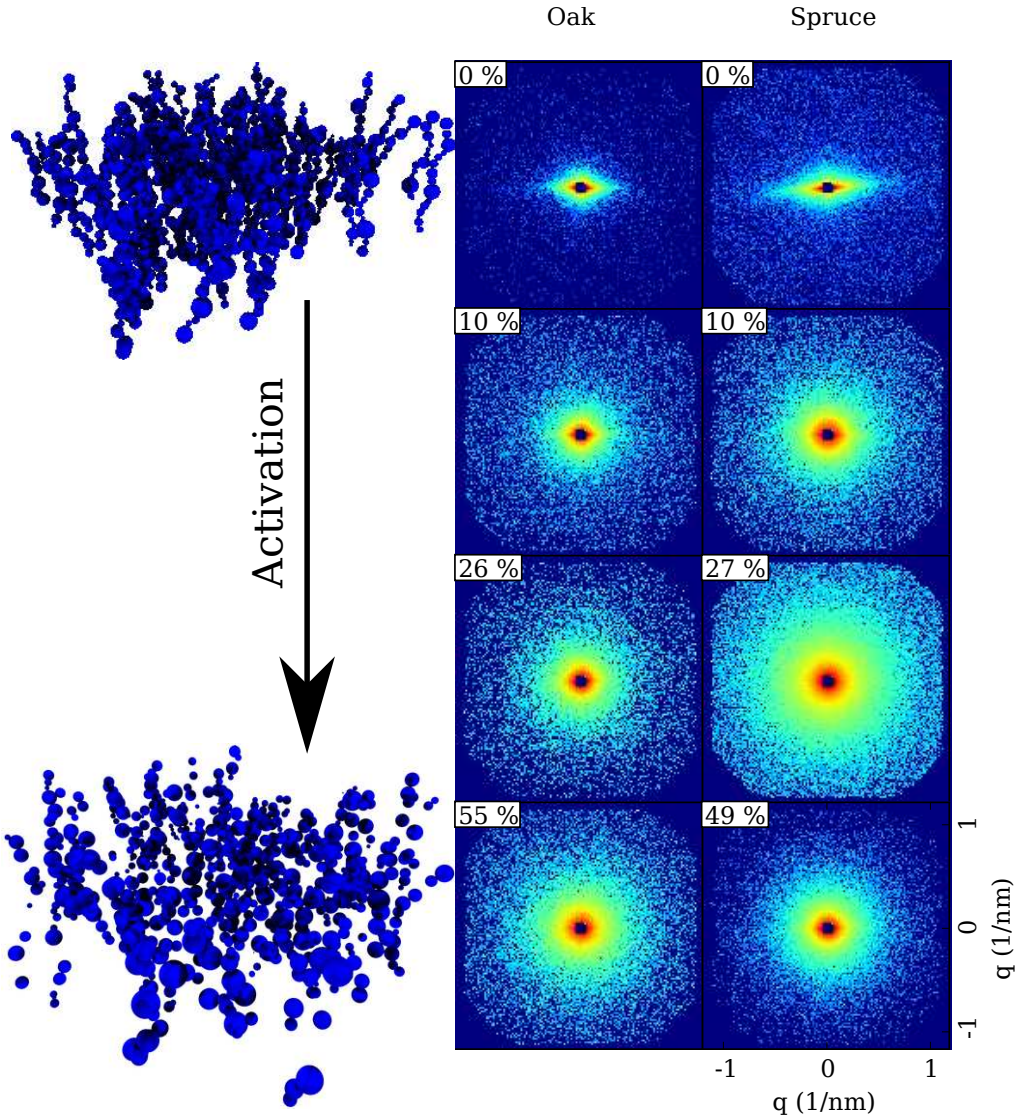

- Horizontal scattering pattern: vertical fibrils
- Decrease in anisotropy: breaking of the fibrils, pore formation
- Characterization of anisotropy: azimuthal scattering curves, sector averaging

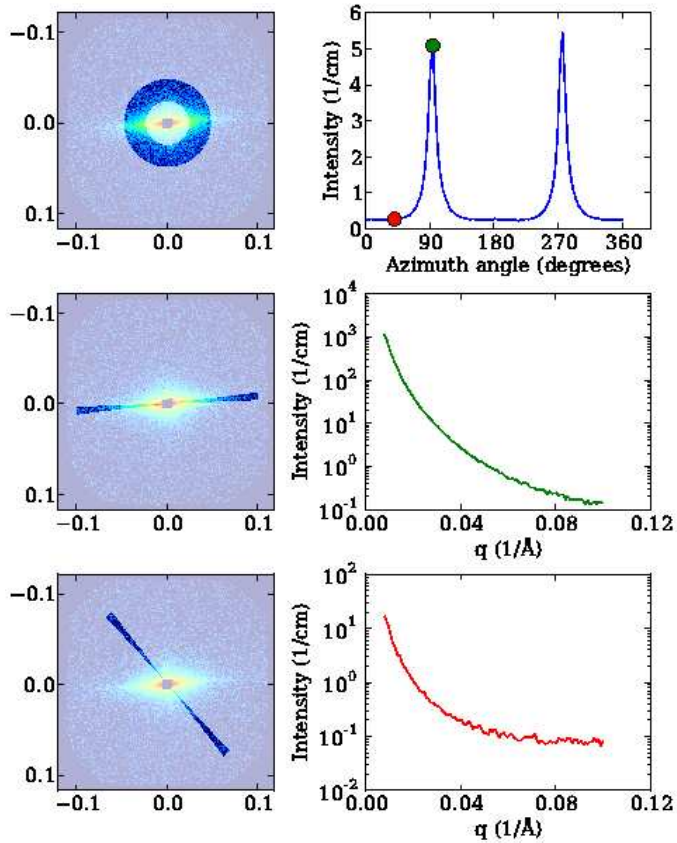

Extent of the anisotropy in real space

Radial sector averages

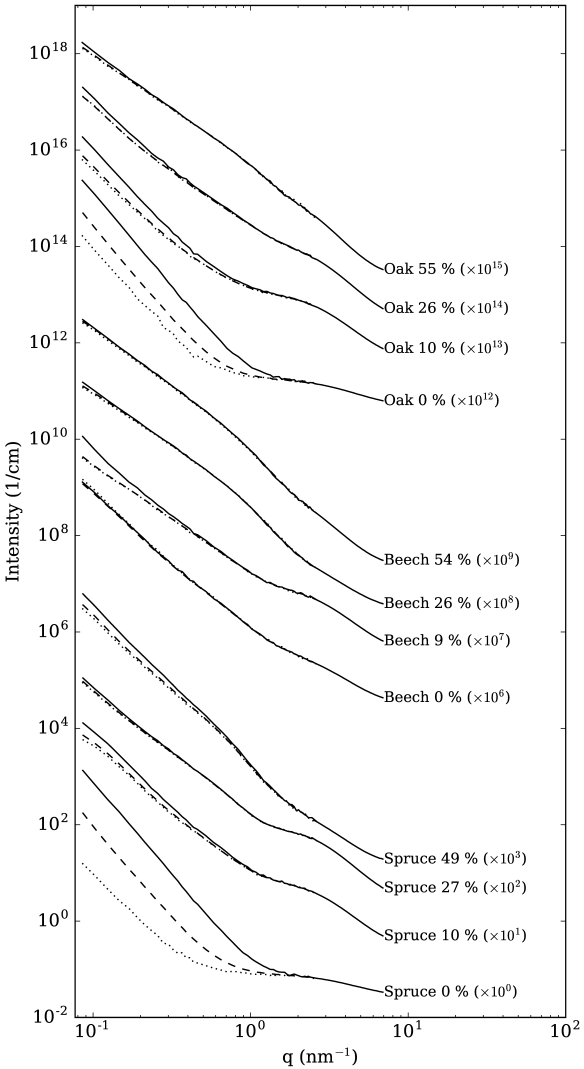

- Radial scattering curves from the scattering patterns
  - Averaging over the full 2π (– – –)
  - Narrowed to the region of the most intensive azimuthal peak (—)
  - Perpendicular to the previous direction ($\cdots$)
- Anisotropy does not appear at small sizes ($q > 2$ nm$^{-1} \rightarrow d < 1.5$ nm)
- Anisotropy decreases with activation
- Power-law functions ($\rightarrow$ fractal dimension) and Guinier regions ($\rightarrow$ radius of gyration)
- Two Guinier regions
  - Small conversion (short activation time): micropores
  - Large conversion (long activation time): mesopores
- Mass fractal $\rightarrow$ surface fractal transition
  - Spruce: surface fractal appears after 49 % burn-off: microcracks
  - Beech: no surface fractal: inherently porous?

Photoluminescent gold-cystein nanocomplexes

- Protein-stabilized supramolecular gold clusters: photoluminescence
- Au-Cys nanocomplex: a simple model for uncovering the stabilizing mechanism

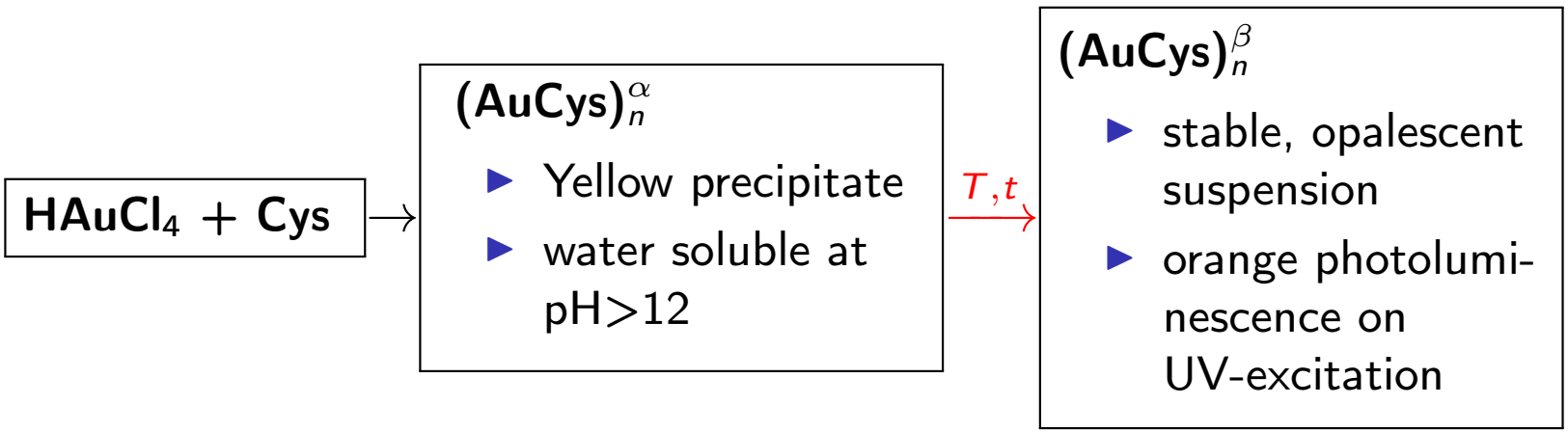

- The speed of transition strongly depends on the temperature of incubation, ranging from a few hours to a day ⇒ time-resolved SAXS on CREDO

Söptei *et. al.* 2015 Coll.Surf.A 470, 8-14.

TRSAXS on the Au-Cys nanocomplex

Incubation at 20 °C

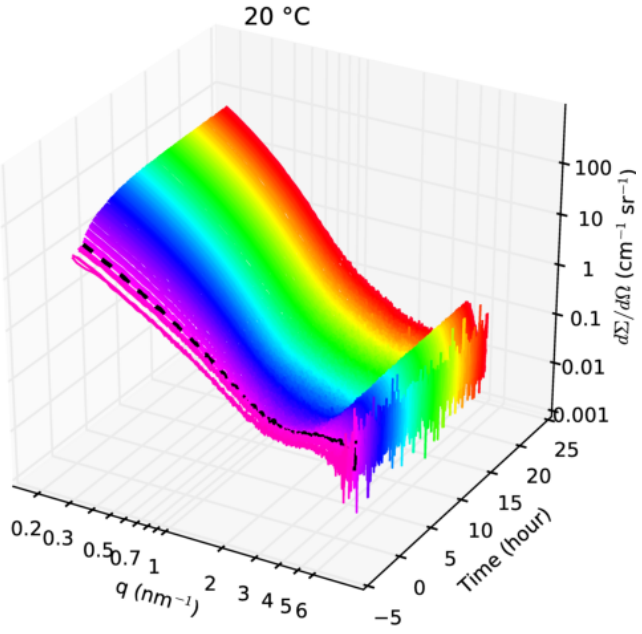

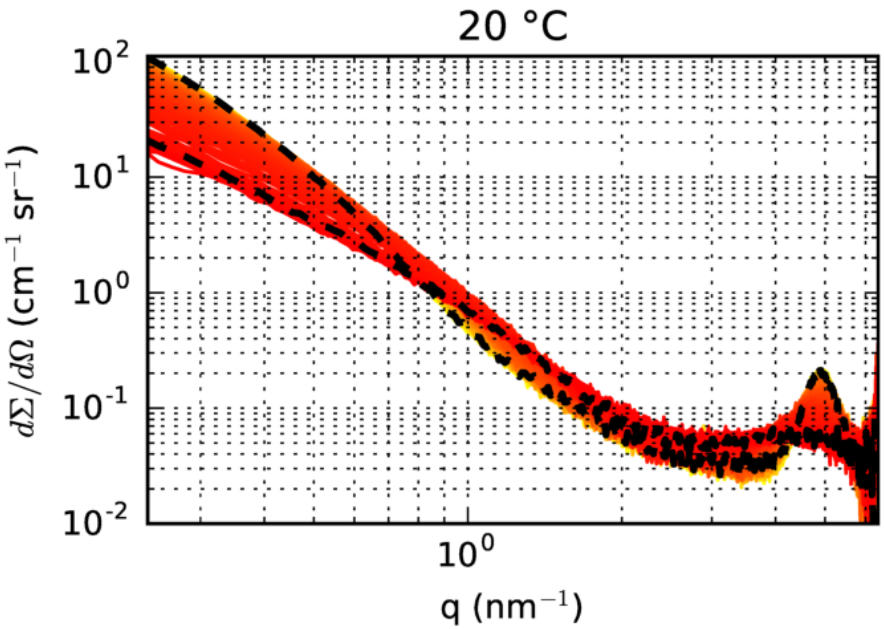

Curvature at small $q \rightarrow$ Guinier

- Objects with well-defined sizes
- Moves left $\rightarrow$ increase in size
- Increasing intensity $\rightarrow$ their number increases
- Starts with $I \propto q^{-2} \rightarrow$ thin lamellae (generalized Guinier)

Peak at the high-q limit

- Periodic structure
- Increasing intensity $\rightarrow$ more perfect periodicity

Automated model fitting

Number of layers and periodicity

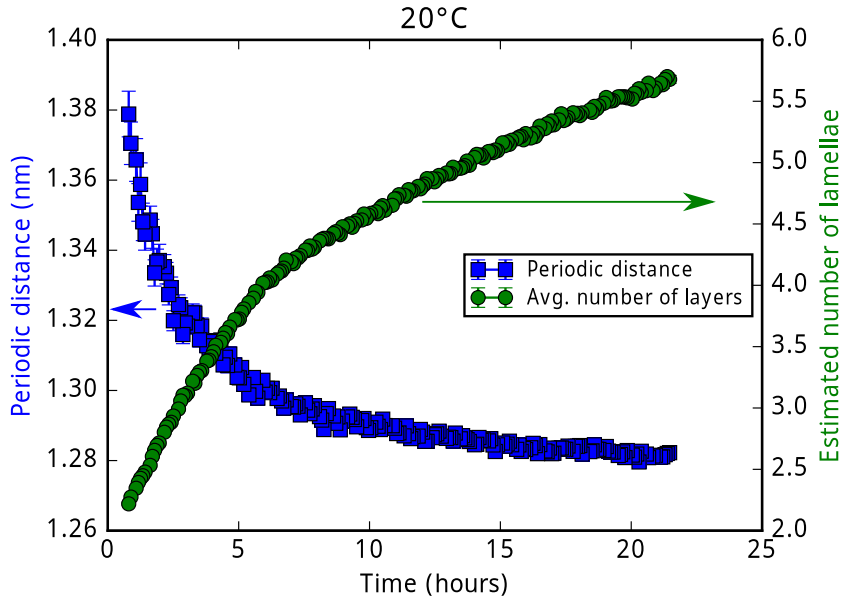

- Guinier approximation for extended lamellae:
  $I_{\text{thickness}} \approx G \cdot q^{-2} e^{-q^2 R_T^2} \quad \rightarrow$
  thickness of the homogeneous lamella:
  $T = \sqrt{12} R_T$
- Final periodic distance: 1.29 nm
- Fine structure of the lamellae: Au layers above each other with ≈ 1.3 nm distance, the Cys molecules acting as spacers
- Well-correlated with the increase of photoluminescence intensity: 0.9208

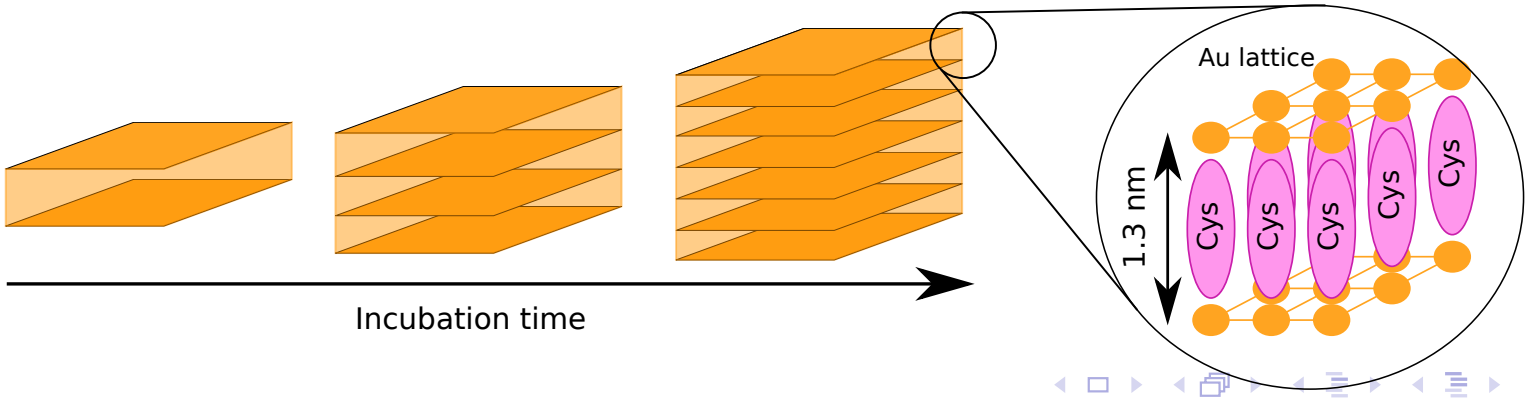

Automated model fitting

Lamellae as seen by TEM

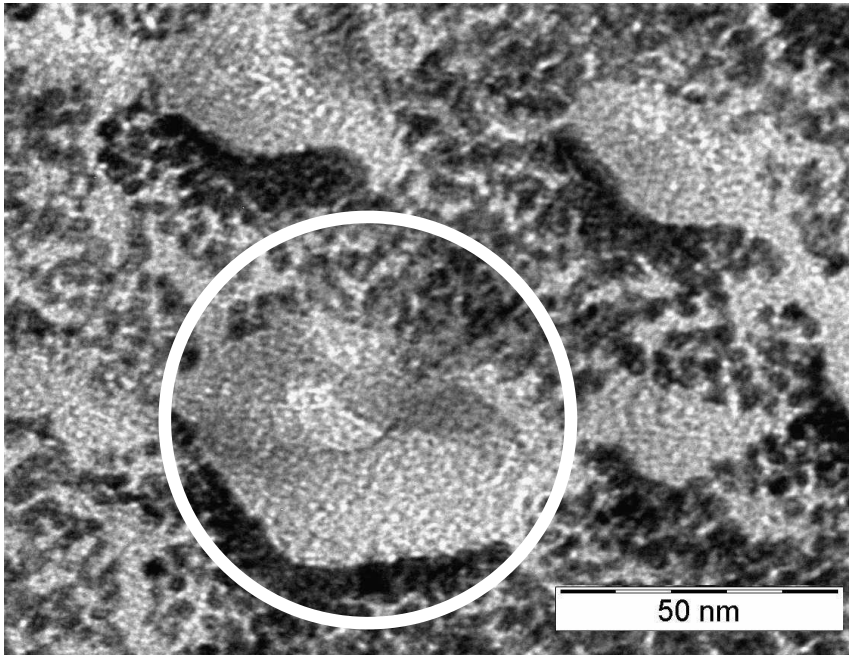

- Guinier approximation for extended lamellae:
  $I_{\text{thickness}} \approx G \cdot q^{-2} e^{-q^2 R_T^2} \quad \rightarrow$
  thickness of the homogeneous lamella:
  $T = \sqrt{12} R_T$
- Final periodic distance: 1.29 nm
- Fine structure of the lamellae: Au layers above each other with ≈ 1.3 nm distance, the Cys molecules acting as spacers
- Well-correlated with the increase of photoluminescence intensity: 0.9208
- FF-TEM measurements: a few nm thick lamellae

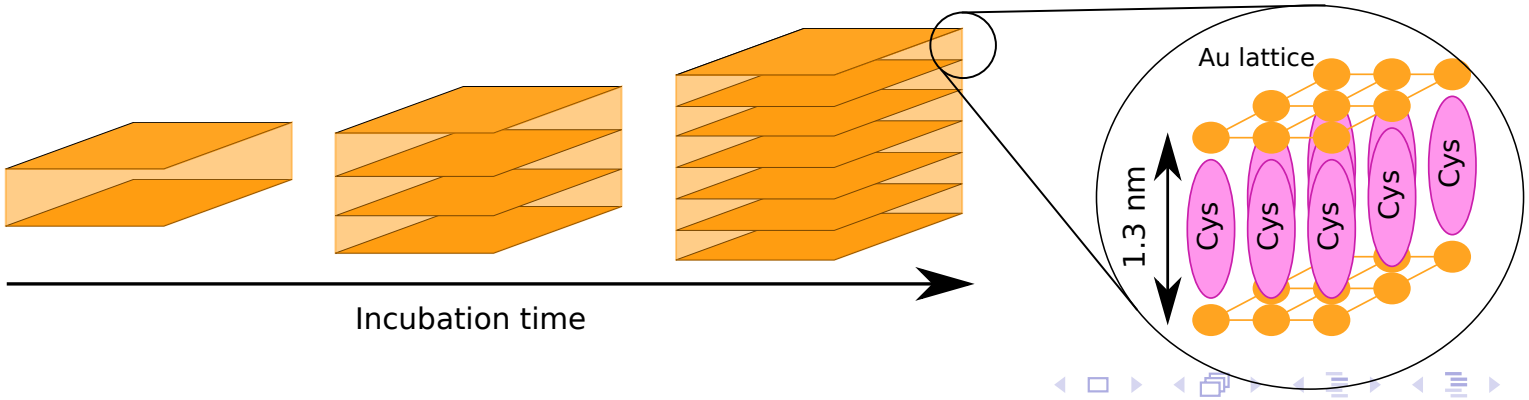

Outline

Size distribution of SiO_2 nanoparticles

Institute for Reference Materials and Measurements, Joint Research Centre of the European Commission: introducing a new SiO_2 particle size standard. Certification of the new material with several SAXS instruments

ERM FD-101b: candidate reference material (CRM)

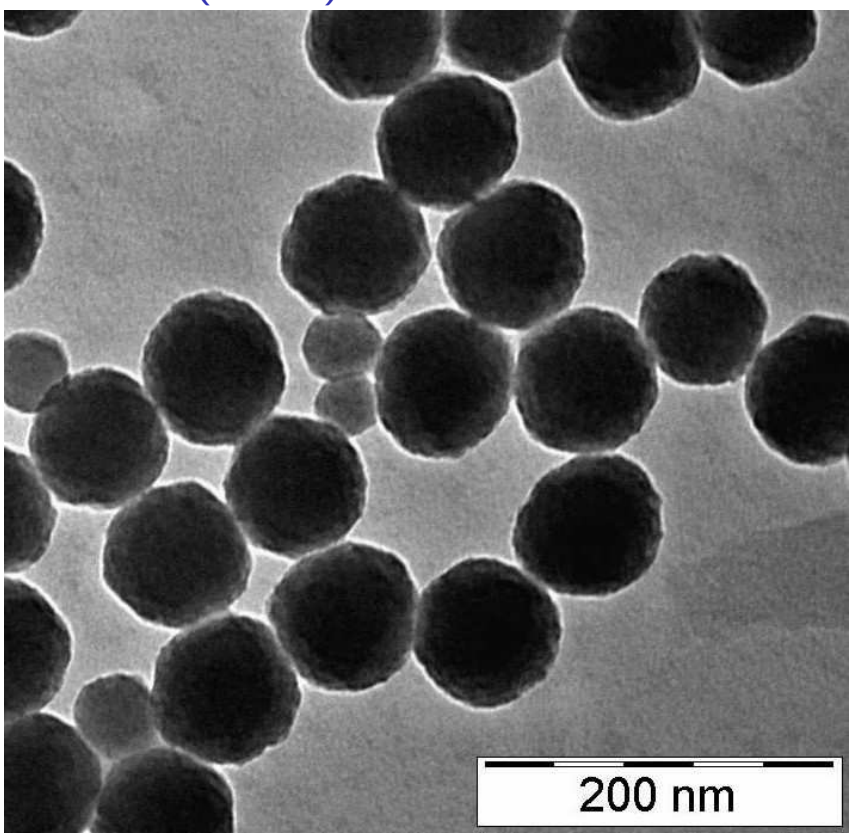

- Methods of size determination:
  1. Guinier fit: $I(q \ll 1/R) \approx I_0 e^{-\frac{q^2 R^2}{5}}$
  2. Fitting of the sphere form factor: $I(q) = \Phi_{\text{sphere}}(q, R) \equiv V_R^2 \left[\frac{3}{(qR)^3} (\sin(qR) - qR\cos(qR)) \right]^2$
  3. Fitting of a sphere distribution: $I(q) = \int_0^\infty p(R) \Phi_{\text{sphere}}(q, R) \mathrm{d}R$
  4. Monte Carlo method: R_i population with w_i statistical weights where $|I(q) - \sum_i w_i \Phi_{\text{sphere}}(q, R_i)|$ is minimized

Size distribution of SiO_2 nanoparticles

Institute for Reference Materials and Measurements, Joint Research Centre of the European Commission: introducing a new SiO_2 particle size standard. Certification of the new material with several SAXS instruments

ERM FD-101b: candidate reference material (CRM)

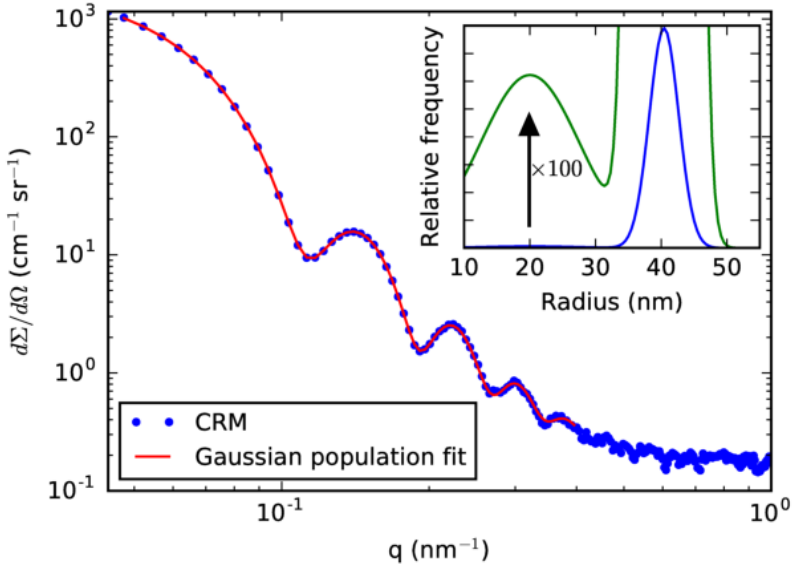

- Methods of size determination:
  1. Guinier fit: $I(q \ll 1/R) \approx I_0 e^{-\frac{q^2R^2}{5}}$
  2. Fitting of the sphere form factor: $I(q) = \Phi_{\text{sphere}}(q, R) \equiv V_R^2 \left[\frac{3}{(qR)^3}(\sin(qR) - qR\cos(qR))\right]^2$
  3. Fitting of a sphere distribution: $I(q) = \int_0^\infty p(R)\Phi_{\text{sphere}}(q, R)\mathrm{d}R$
  4. Monte Carlo method: R_i population with w_i statistical weights where $|I(q) - \sum_i w_i \Phi_{\text{sphere}}(q, R_i)|$ is minimized

Size distribution of SiO_2 nanoparticles

Institute for Reference Materials and Measurements, Joint Research Centre of the European Commission: introducing a new SiO_2 particle size standard. Certification of the new material with several SAXS instruments

Monte Carlo size determination

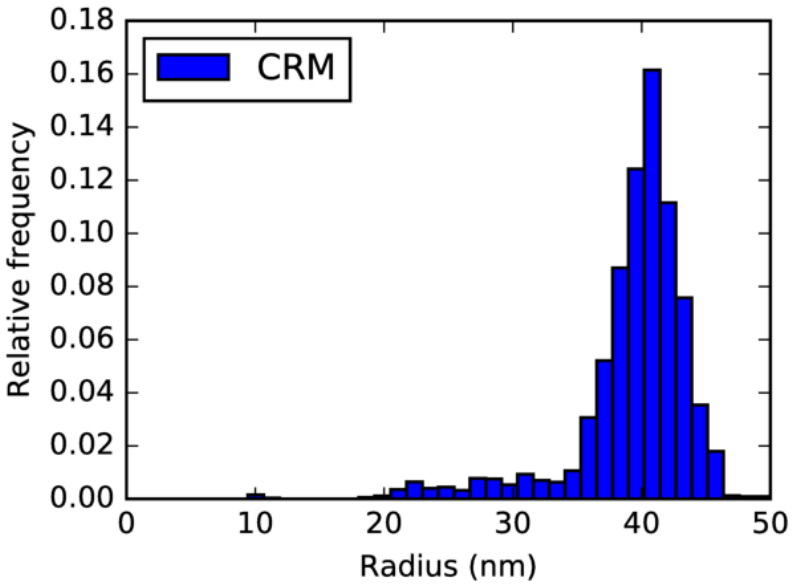

- Methods of size determination:
  1. Guinier fit: $I(q \ll 1/R) \approx I_0 e^{-\frac{q^2 R^2}{5}}$
  2. Fitting of the sphere form factor: $I(q) = \Phi_{\text{sphere}}(q, R) \equiv V_R^2 \left[\frac{3}{(qR)^3} (\sin(qR) - qR\cos(qR)) \right]^2$
  3. Fitting of a sphere distribution: $I(q) = \int_0^\infty p(R) \Phi_{\text{sphere}}(q, R) \mathrm{d}R$
  4. Monte Carlo method: R_i population with w_i statistical weights where $|I(q) - \sum_i w_i \Phi_{\text{sphere}}(q, R_i)|$ is minimized

Size distribution of SiO_2 nanoparticles

Institute for Reference Materials and Measurements, Joint Research Centre of the European Commission: introducing a new SiO_2 particle size standard. Certification of the new material with several SAXS instruments

Monte Carlo size determination

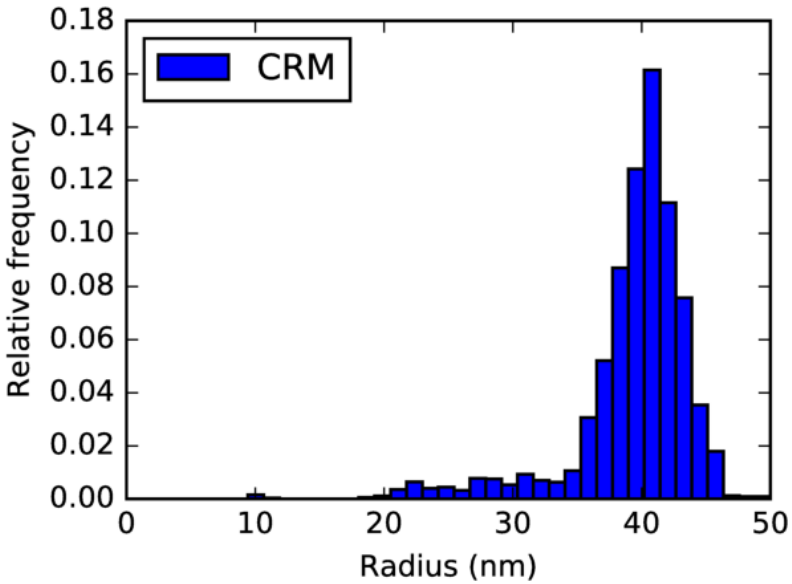

- Methods of size determination:
  1. Guinier fit: $I(q \ll 1/R) \approx I_0 e^{-\frac{q^2R^2}{5}}$
  2. Fitting of the sphere form factor: $I(q) = \Phi_{\text{sphere}}(q, R) \equiv V_R^2 \left[\frac{3}{(qR)^3}\left(\sin(qR) - qR\cos(qR)\right)\right]^2$
  3. Fitting of a sphere distribution: $I(q) = \int_0^\infty p(R)\Phi_{\text{sphere}}(q, R)\mathrm{d}R$
  4. Monte Carlo method: R_i population with w_i statistical weights where $|I(q) - \sum_i w_i \Phi_{\text{sphere}}(q, R_i)|$ is minimized

A favourable side-effect: CREDO has been certified by IRMM for nanoparticle size distribution determination

Biological Small-Angle X-ray Scattering

BioSAXS

- Biorelevant macromolecules
- Mainly size- and shape determination assuming particles of homogeneous electron density
- Key parameters: R_g, $I_0 \equiv \lim_{q \to 0} I(q)$
- Information to be obtained:
  - Size, (low resolution) shape, volume and molecular mass of the protein
  - Flexibility/folding state (folded/disordered)
  - Validation of crystal structures
  - Aligning the relative positions of known domains

Drawbacks / caveats

- Low scattering contrast $\Rightarrow$ bad signal/noise ratio
- Dilute sample (otherwise Guinier approximation breaks down)
- Purified sample (esp. contaminating large molecules)
- Monodisperse sample (avoid oligomerization, aggregation)
- Featureless scattering curve: danger of "overfitting"
- Uncertainties of background subtraction (solvent scattering)
- Phase problem $\Rightarrow$ the uniqueness of the determined shape

The BioSAXS method

- Well-established and validated algorithms and methods available
- Basic assumptions: the protein solution is a *monodisperse* population of *independent*, *homogeneous* nanoparticles

  independent: no interparticle interference, Guinier approximation holds

  monodisperse: no oligomerization, no aggregation

  homogeneous: simple shape fitting; SAXS is blind on the atomic length-scale!

Interpretation of BioSAXS measurements

- Guinier approximation: $I(q \ll R_g) \propto I_0 e^{-\frac{q^2 R_g^2}{3}}$; $I_0 = (\Delta\rho)^2 V^2$.
- Porod invariant: $Q \equiv \frac{1}{2\pi^2} \int_0^\infty q^2 I(q) \mathrm{d}q = 2\pi^2 (\Delta\rho)^2 V$
- Porod volume: $V_{\mathrm{Porod}} = 2\pi^2 I_0 / Q$
- First steps:
  1. Subtraction of the solvent background (corrected by the volume fraction of the protein)
  2. Guinier fit $\rightarrow I_0, R_g$
  3. Porod invariant $\rightarrow V_{\mathrm{Porod}}$
  4. Inverse Fourier: $I(q) \rightarrow p(r)$ pair distance distribution function (PDDF)
  5. I_0, R_g can be obtained from $p(r)$:

$$I_0 = \int_0^\infty p(r) \mathrm{d}r; \qquad R_g^2 = \frac{\int_0^\infty p(r) r^2 \mathrm{d}r}{2 \int_0^\infty p(r) \mathrm{d}r}$$

  6. Compare the I_0 and R_g obtained from the two methods
  7. Further interpretation...
- ATSAS: software suite for BioSAXS data processing and interpretation (EMBL Hamburg, Research Group of Dmitri Svergun)

The Kratky plot

- High-q part of the scattering of a polimer chain following Gaussian statistics: $I(q \to \infty) \propto \frac{2}{q^2 R_g^2}$
- Kratky plot: $q^2 I$ - q. Behaviour in the $q \to \infty$ limit:
  - Folded proteins ($I \propto q^{-4}$): tends to 0
  - Disordered proteins ($I \propto q^{-2}$): constant or divergent

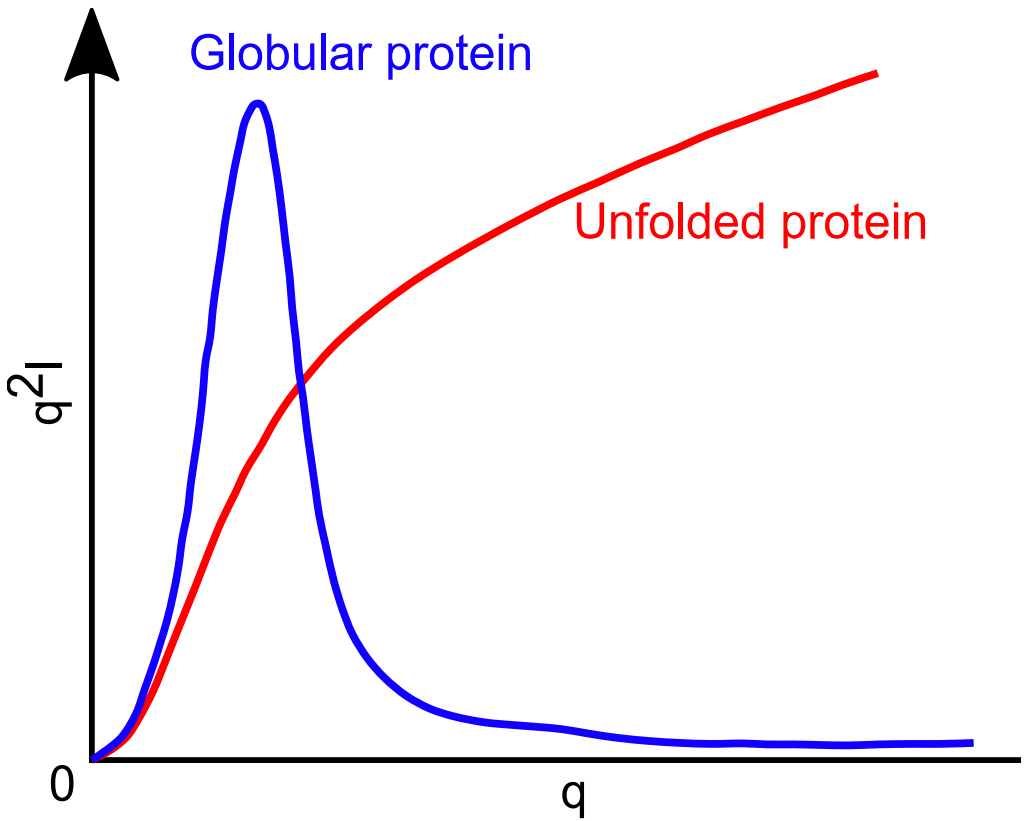

Source: https://www-ssrl.slac.stanford.edu/~saxs/analysis/assessment.htm

Protein shape fitting from small-angle scattering

Fitting of geometrical shapes to scattering curves or PDDFs

- BODIES program (part of ATSAS)
- Ball, hollow sphere, ellipsoid, dumbbell etc.
- Very few parameters

Dummy atom model (DAM)

- Constructing the shape from tightly packed (fcc or hcp lattice) spherical building blocks
- Monte Carlo algorithm
  1. Random configuration
  2. Small, random modification of the configuration (add/remove a unit)
  3. Calculate scattering
  4. Compare the measured and calculated scattering
     - Better fit: keep the change
     - Worse fit: drop the change (or keep it with a low probability)
  5. Repeat from step #2 until needed
- Many parameters: possible ambiguity of the results

Protein shape fitting from small-angle scattering

Fitting of geometrical shapes to scattering curves or PDDFs

- BODIES program (part of ATSAS)
- Ball, hollow sphere, ellipsoid, dumbbell etc.
- Very few parameters

Dummy atom model (DAM)

- Constructing the shape from tightly packed (fcc or hcp lattice) spherical building blocks
- Monte Carlo algorithm
  1. Random configuration
  2. Small, random modification of the configuration (add/remove a unit)
  3. Calculate scattering
  4. Compare the measured and calculated scattering
     - Better fit: keep the change
     - Worse fit: drop the change (or keep it with a low probability)
  5. Repeat from step #2 until needed
- Many parameters: possible ambiguity of the results

Lysozyme – A “typical” BioSAXS experiment

Crystal structure

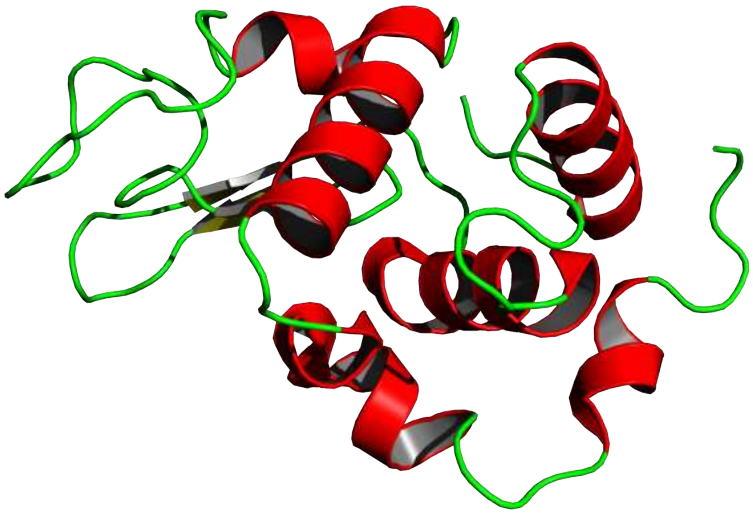

- Well-known protein (“veterinary horse”)

Lysozyme – A “typical” BioSAXS experiment

Effect of concentration

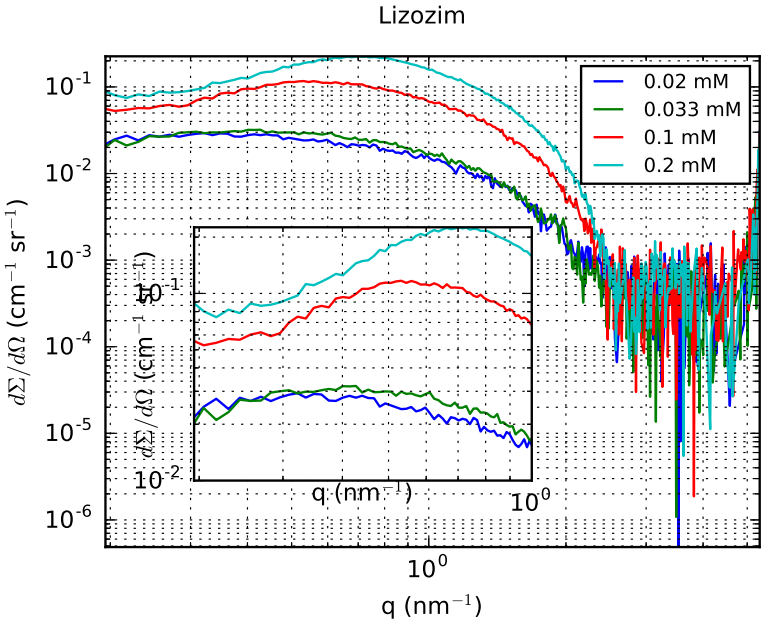

- Well-known protein (“veterinary horse”)
- Correlation peak
  - Caused by el.stat. repulsion
  - Radius of gyration cannot be determined
  - How to get rid of it?
    - Dilution

Lysozyme – A "typical" BioSAXS experiment

Effect of ionic strength

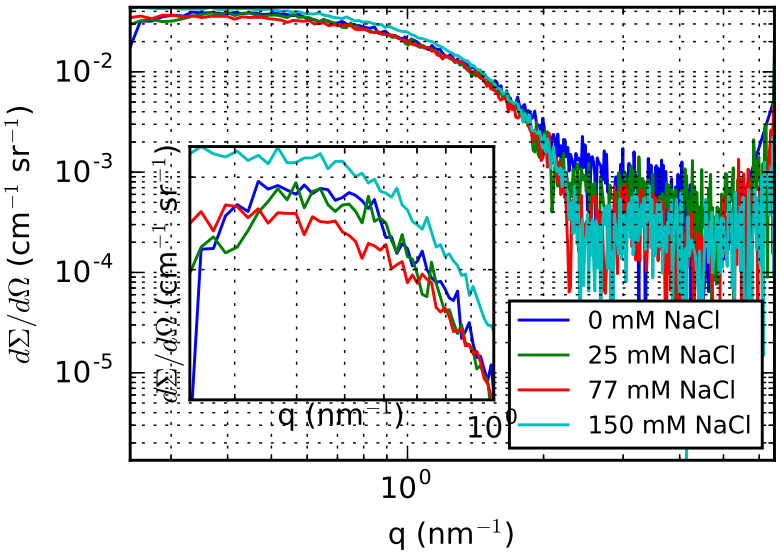

- Well-known protein ("veterinary horse")
- Correlation peak
  - Caused by el.stat. repulsion
  - Radius of gyration cannot be determined
  - How to get rid of it?
    - Dilution
    - Salting (screening the repulsion)

Lysozyme – A "typical" BioSAXS experiment

Guinier plot

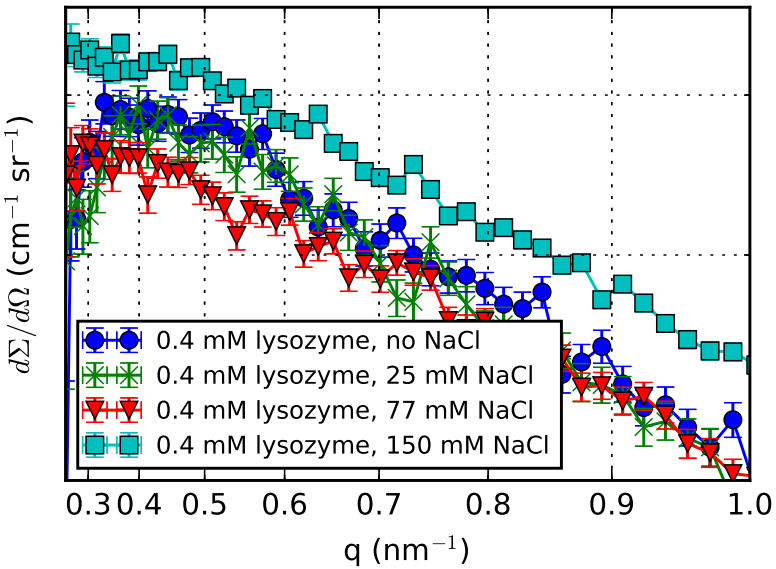

- Well-known protein ("veterinary horse")
- Correlation peak
  - Caused by el.stat. repulsion
  - Radius of gyration cannot be determined
  - How to get rid of it?
    - Dilution
    - Salting (screening the repulsion)
- Guinier plot ($\log I$ vs. q^2): assessing the $I \propto \exp\left(-q^2 R_g^2/3\right)$ shape

Lysozyme – A "typical" BioSAXS experiment

Kratky plot

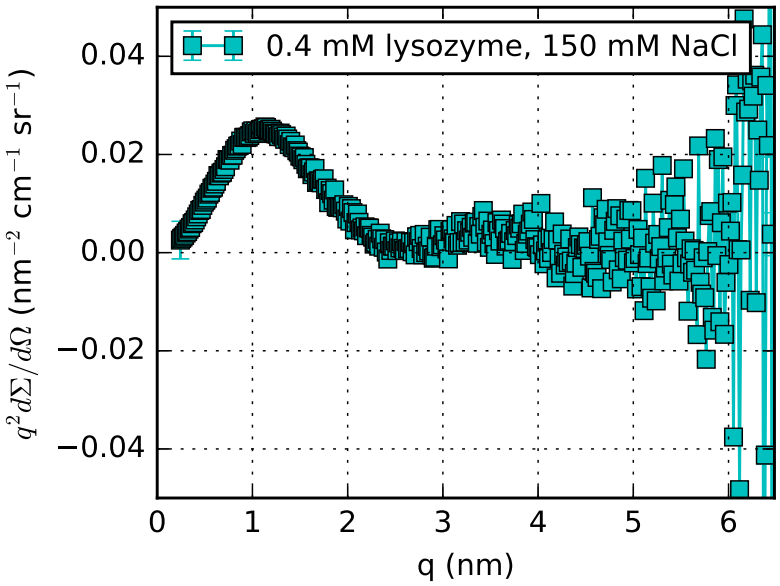

- Well-known protein ("veterinary horse")
- Correlation peak
  - Caused by el.stat. repulsion
  - Radius of gyration cannot be determined
  - How to get rid of it?
    - Dilution
    - Salting (screening the repulsion)
- Guinier plot ($\log I$ vs. q^2): assessing the $I \propto \exp\left(-q^2 R_g^2/3\right)$ shape
- Kratky plot ($q^2 I$ vs. q): folded protein

The shape of lysozyme

„Dummy atom model" – coarse-grained description

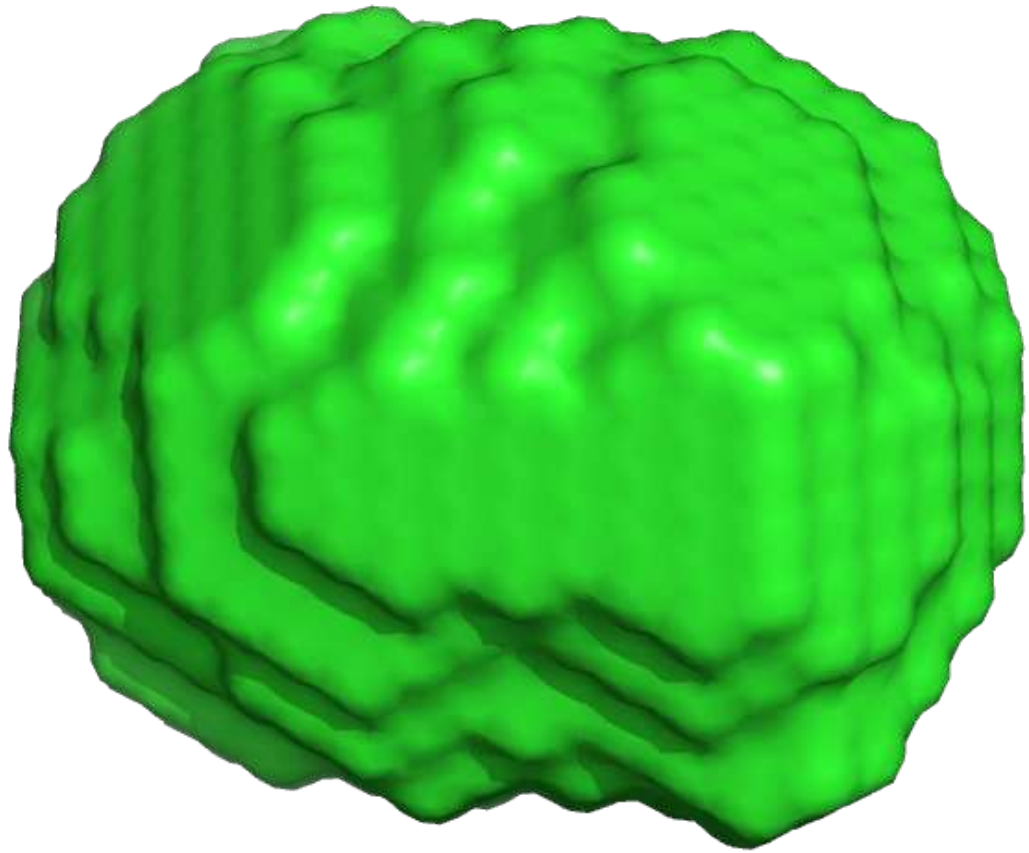

The shape of lysozyme

„Dummy atom model" – coarse-grained description

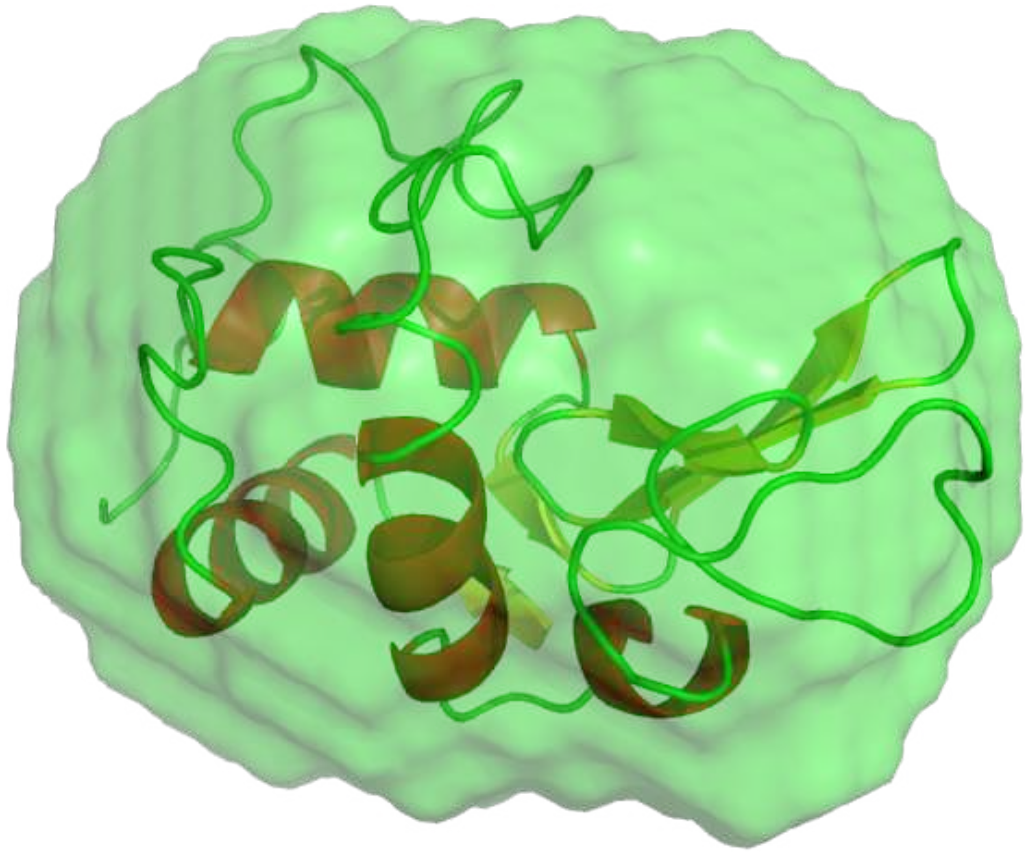

Good agreement with the crystal structure!

Calmodulin

- Highly abundant plasma protein of eukaryotic cells (≈ 1 %)
- Key element of Ca^{2+}-induced signal pathways

Apo (Ca^{2+}-free) conformation (MX)

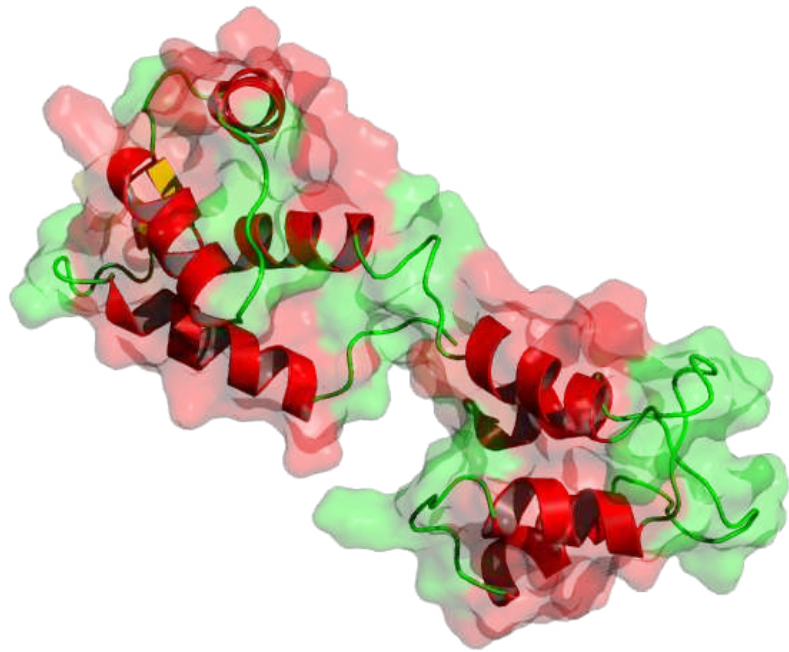

Envelope: Van der Waals surface

Calmodulin

- Highly abundant plasma protein of eukaryotic cells (≈ 1 %)
- Key element of Ca^{2+}-induced signal pathways
- Changes shape on Ca^{2+} binding
  - The "EF-hand" motifs open in both end-domains: hydrophobic pockets open up
  - End domains are displaced
  - Secondary structure of the linker part: loop $\rightarrow$ helix (known crystallization artefact!)

Ca^{2+}-bound conformation (MX)

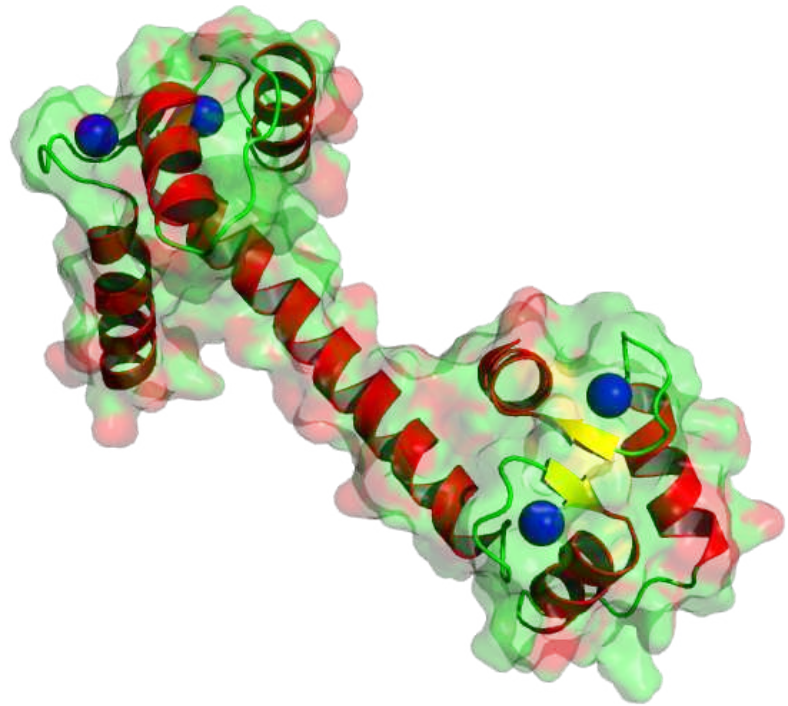

Envelope: Van der Waals surface

Calmodulin – SAXS results

Scattering curves

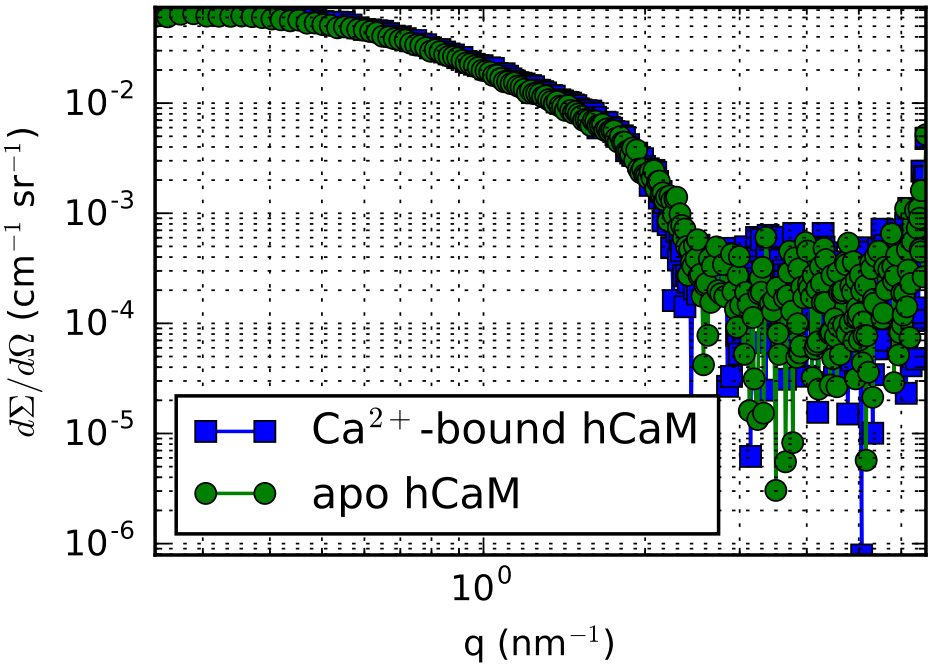

- Very similar scattering curves
- Scattering curves: dumbbell shape

Calmodulin – SAXS results

Guinier plot

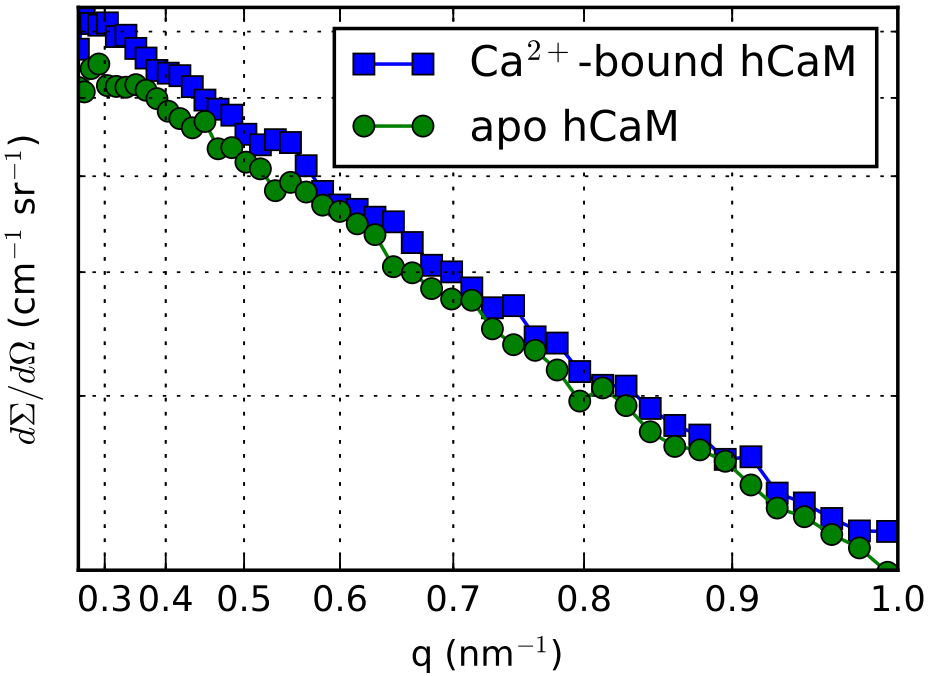

- Very similar scattering curves
- Scattering curves: dumbbell shape
- Similar radii of gyration

Calmodulin – SAXS results

Kratky plot

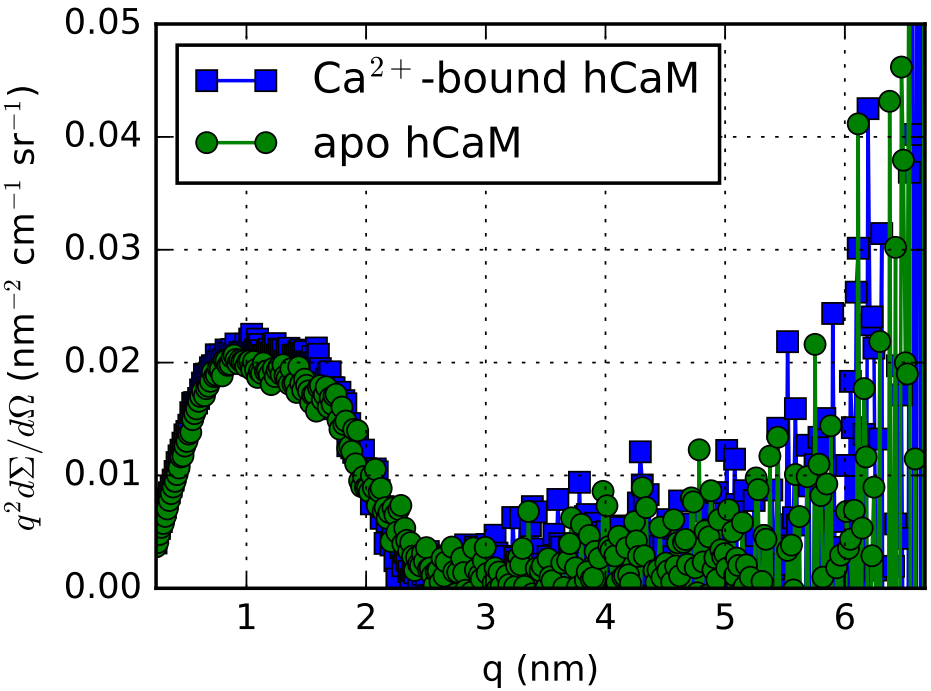

- Very similar scattering curves
- Scattering curves: dumbbell shape
- Similar radii of gyration
- Partially disordered (linker part?)

Calmodulin – SAXS results

DAM: apo conformation

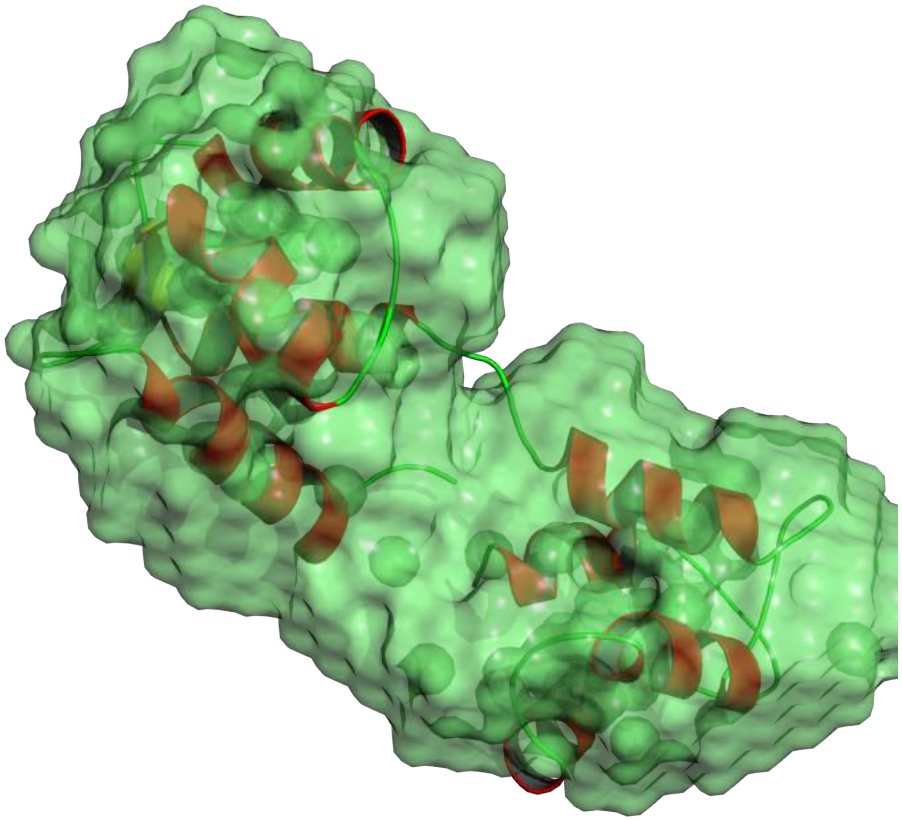

- Very similar scattering curves
- Scattering curves: dumbbell shape
- Similar radii of gyration
- Partially disordered (linker part?)
- Dummy atom model:
  - Dumbbell shape
  - Apo conformation more “loose”

Calmodulin – SAXS results

DAM: Ca^{2+}-bound conformation

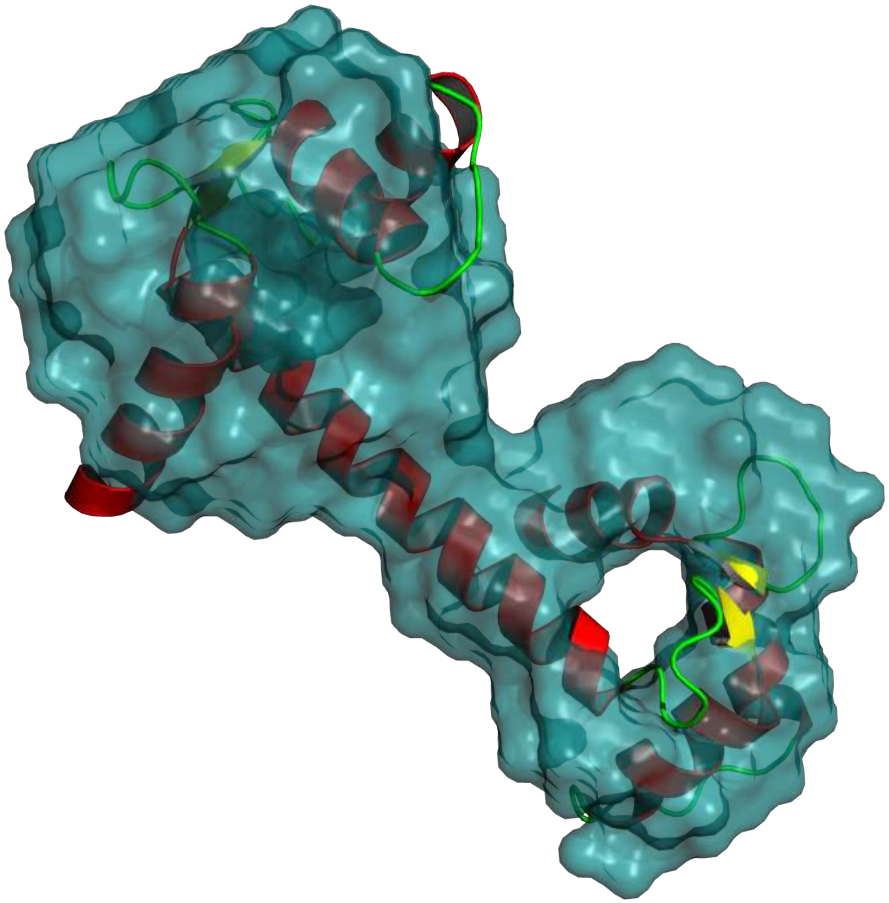

- Very similar scattering curves
- Scattering curves: dumbbell shape
- Similar radii of gyration
- Partially disordered (linker part?)
- Dummy atom model:
  - Dumbbell shape
  - Apo conformation more "loose"
  - Ca^{2+} binding makes the structure more rigid
  - Differences from the crystal structure: crystallization artefacts?

Reliability of dummy atom models

- Phase problem!
- Methods to improve reliability
  - Several candidate shapes from multiple runs of DAMMIF
  - Screening the candidates with DAMSEL
  - Average the remaining shapes with DAMAVER
  - Refine the average shape with DAMMIN

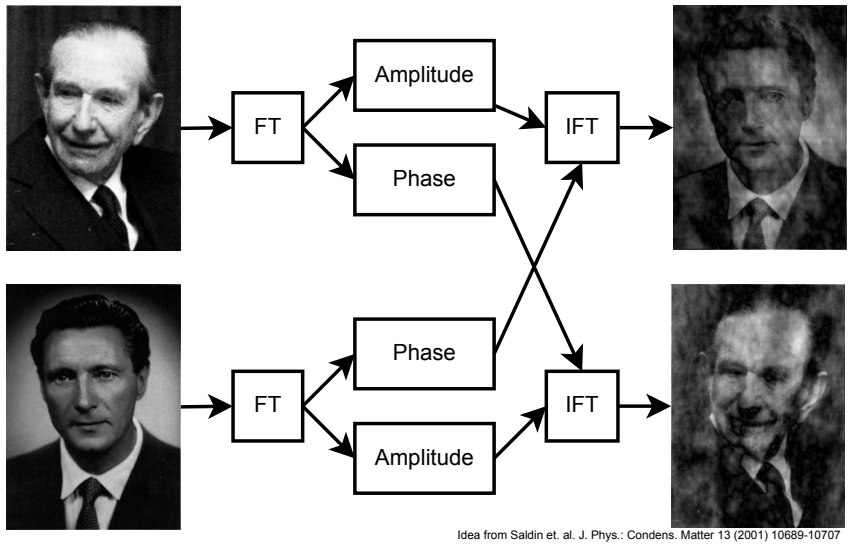

Idea from Saldin et. al. J. Phys.: Condens. Matter 13 (2001) 10689-10707

Reliability of dummy atom models

- Phase problem!
- Methods to improve reliability
  - Several candidate shapes from multiple runs of DAMMIF
  - Screening the candidates with DAMSEL
  - Average the remaining shapes with DAMAVER
  - Refine the average shape with DAMMIN
- Quantification of the ambiguity (AMBIMETER)

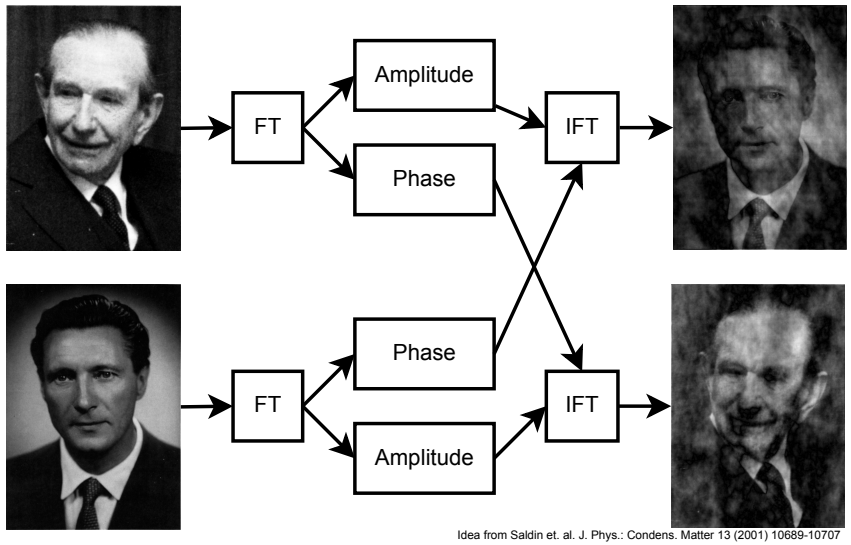

Idea from Saldin et. al. J. Phys.: Condens. Matter 13 (2001) 10689-10707

Reliability of dummy atom models

- Phase problem!
- Methods to improve reliability
  - Several candidate shapes from multiple runs of DAMMIF
  - Screening the candidates with DAMSEL
  - Average the remaining shapes with DAMAVER
  - Refine the average shape with DAMMIN
- Quantification of the ambiguity (AMBIMETER)
  - A library has been made from *all possible shapes*
  - Dimensionless scattering curves for the library elements: $I(q)/I_0$ vs. qR_g

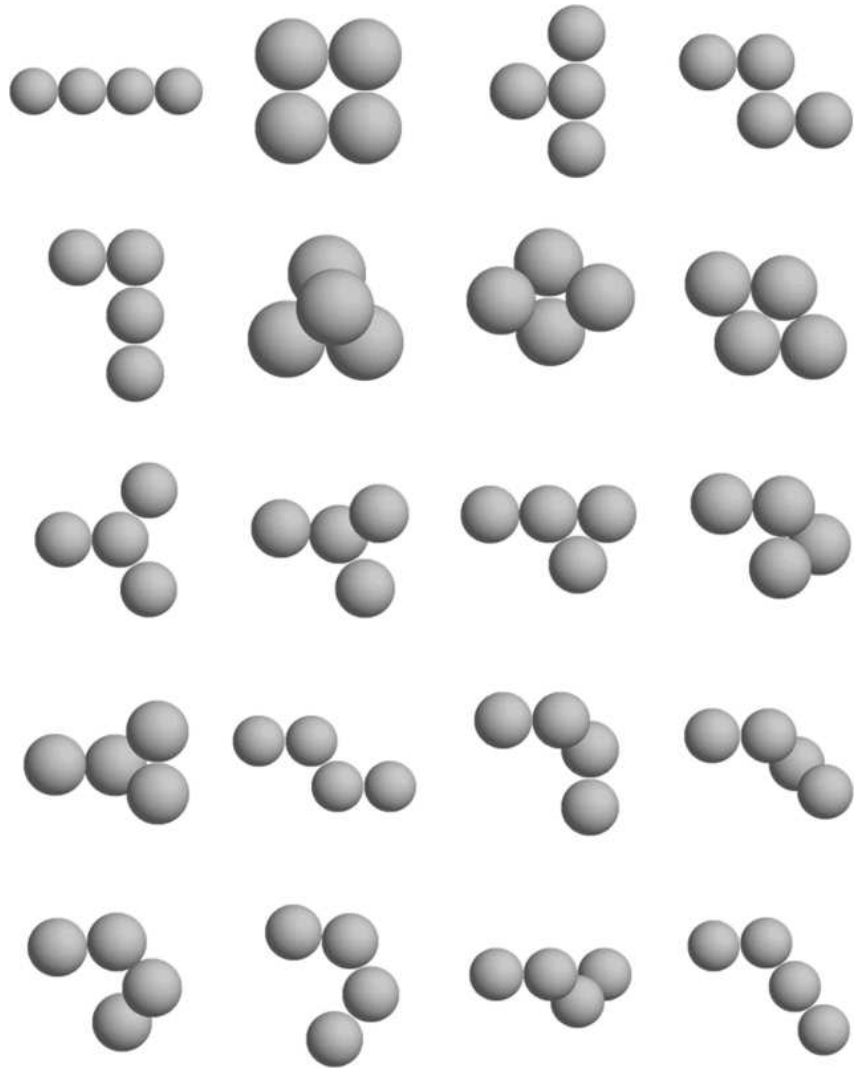

Petoukhov & Svergun, Acta Crystallographica D 2015, 71(5), 1051-1058

Reliability of dummy atom models

- Phase problem!
- Methods to improve reliability
  - Several candidate shapes from multiple runs of DAMMIF
  - Screening the candidates with DAMSEL
  - Average the remaining shapes with DAMAVER
  - Refine the average shape with DAMMIN
- Quantification of the ambiguity (AMBIMETER)
  - A library has been made from *all possible shapes*
  - Dimensionless scattering curves for the library elements: $I(q)/I_0$ vs. qR_g
  - Find number of those library elements where the curve is compatible with the measured one

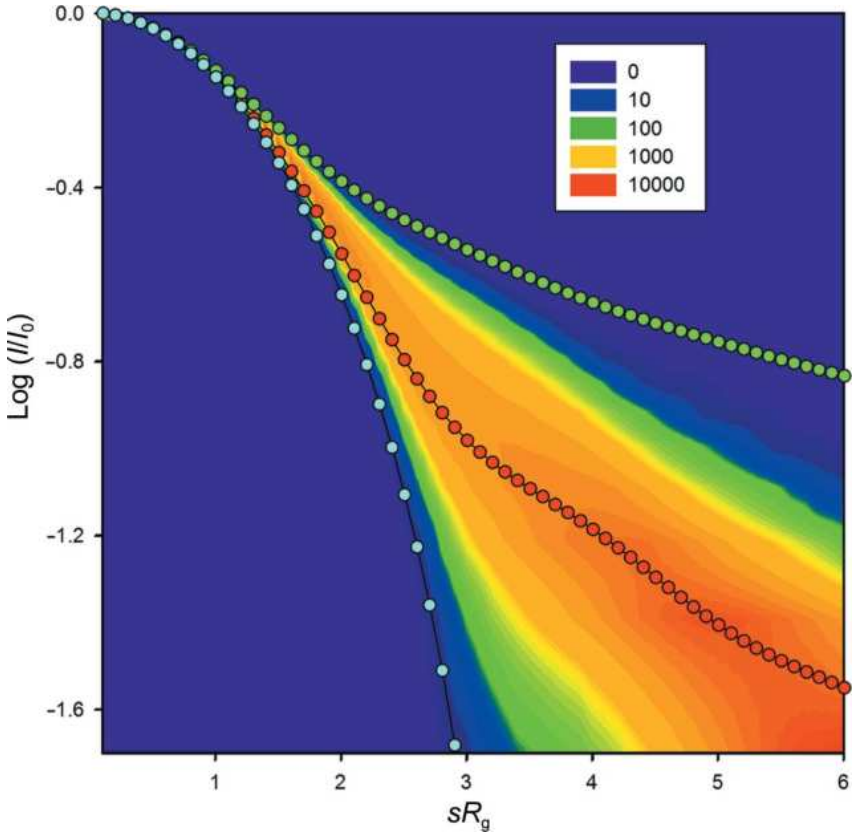

Petoukhov & Svergun, Acta Crystallographica D 2015, 71(5), 1051-1058

Reliability of dummy atom models

- Phase problem!
- Methods to improve reliability
  - Several candidate shapes from multiple runs of DAMMIF
  - Screening the candidates with DAMSEL
  - Average the remaining shapes with DAMAVER
  - Refine the average shape with DAMMIN
- Quantification of the ambiguity (AMBIMETER)
  - A library has been made from *all possible shapes*
  - Dimensionless scattering curves for the library elements: $I(q)/I_0$ vs. qR_g
  - Find number of those library elements where the curve is compatible with the measured one
  - Lysozyme: 1; apo calmodulin: 422; Ca^{2+}-bound calmodulin: 417

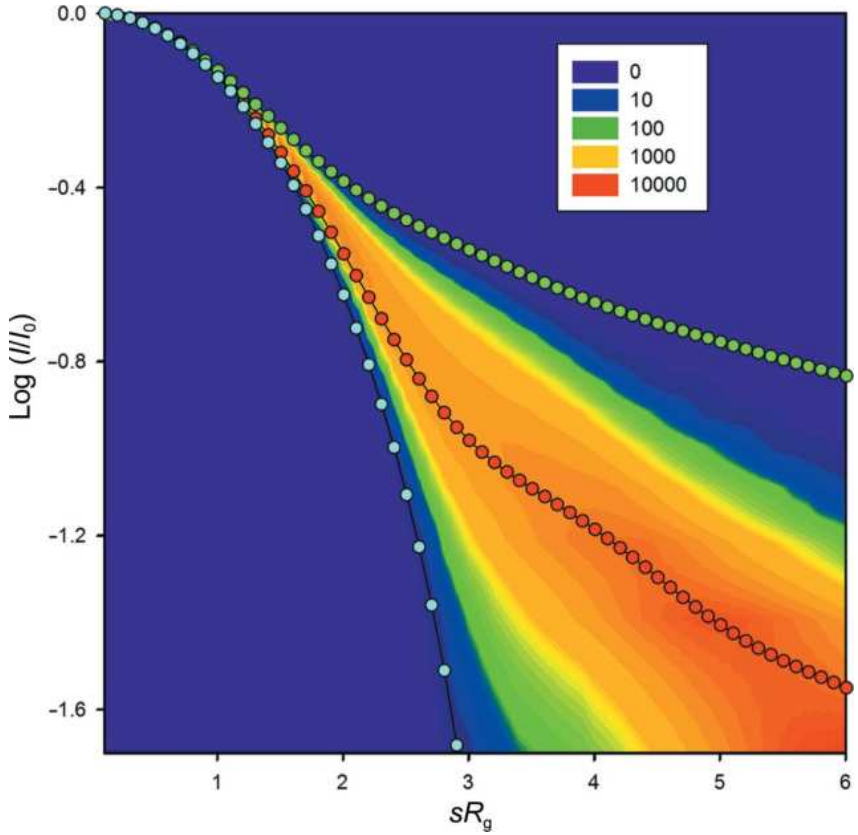

Petoukhov & Svergun, Acta Crystallographica D 2015, 71(5), 1051-1058

Outline

Literature and software

Software

- SASFit: model fitting
- ATSAS: BioSAXS data handling, R_G, PDDF calculation, dummy atom fitting etc.
- SANSView: plotting, model fitting

Literature

- Boualem Hammouda: *Probing Nanoscale Structures: The SANS Toolbox* (http://www.ncnr.nist.gov/staff/hammouda/the_SANS_toolbox.pdf)
- J. Kohlbrecher, I. Breßler: *SASFit manual* (http://kur.web.psi.ch/sans1/SANSSoft/sasfit.html)
- L. A. Feigin és D. I. Svergun: *Structure Analysis by Small-Angle X-Ray and Neutron Scattering* (http://www.embl-hamburg.de/biosaxs/reprints/feigin_svergun_1987.pdf)

Summary

Interpretation of SAXS results

- Multilamellar vesicles and ordered lipid systems: determination of the periodic repeat distance
- Sterically stabilized vesicles: the radial electron density distribution of the phospholipid bilayer
- Micelles and bicelles: shape, core-shell model parameters
- Activated carbons: anisotropy, fractal properties
- Gold-cysteine nanocomplex: the time evolution of the photoluminescent nanostructure
- SiO_2 nanoparticles (repeated): size, size distribution
- BioSAXS: determination of the size, shape and flexibilitx of proteins *in solution*

Acknowledements

The experimental results presented in this lecture could not have been made without the contributions (sample preparations, ideas etc.) of the following people:

- Attila Bóta
- Judith Mihály
- Zoltán Varga
- Andrea Jónás
- Andrea Bodor
- Erika Dudás
- Tünde Juhász
- Balázs Söptei

Thank you for your attention!